Final Report

Scavenger Well Operation Model to Assist BRWC to Identify Cost-Effective Approaches to Stop Saltwater Intrusion toward the BRWC Water Wells in the "1,500-Foot" Sand of the Baton Rouge Area

Submitted to

Eugene H. Owen
Executive Chairman
Baton Rouge Water Company
8755 Goodwood Boulevard
Baton Rouge, LA 70806

Don C. Dial
Director
Capital Area Ground Water
Conservation Commission
3535 South Sherwood Forest Blvd.,
Suite 129
Baton Rouge, LA 70816

Prepared by

Frank T.-C. Tsai, Ph.D., P.E.
Louisiana State University
Civil and Environmental Engineering Department
3418G Patrick F. Taylor Hall
Baton Rouge, LA 70803-6405
Tel: (225) 578-4246
Fax: (225) 578-4945
Email: ftsai@lsu.edu

January 28, 2011

Acknowledgements

Contents

Executive Summary

The project evaluated the efficiency of using scavenger wells to stop saltwater approaching water wells at Lula pump station that were screened at the "1,500-foot" sand. Undesirable chloride concentrations were detected at few water wells at Lula pump station. This poses an urgent concern that saltwater, which is initially restrained at the south of the Baton Rouge fault, may have crossed the fault, encroached in the "1,500-foot" sand, and arrived near the water wells at Lula pump station. Scavenger wells are small extraction wells to be placed a certain distance in front of water wells to capture saltwater. The project develops a scavenger well operation (SWOP) model to optimize scavenging designs that determine the number of wells, well locations and extraction rates to effectively capture saltwater. In the first phase, a saltwater intrusion model was developed and calibrated for a 65-year period, from 1/1/1945 to 12/31/2009. The simulation result clearly revealed a unique saltwater intrusion pattern in the "1,500-foot" sand. The apex of the saltwater front in the early years was moving northward toward the water wells at Government pump station, but eventually leaned to the west toward the water wells at Lula pump station. This is a discovery since it was long believed that saltwater would first arrive at water wells at Government pump station and then N. 45th pump station (e.g., Rollo, 1969). In the second phase, saltwater intrusion was predicted under current pumpages for the next 50 years, from 1/1/2010 to 12/31/2060. Chloride concentration at EB-658 (Lula-19) would continue to rise and would reach around 750 mg/L on 1/1/2035 and around 1,500 mg/L on 1/1/2060. In 50 years, water wells at Government pump station would face the same saltwater intrusion issue as now. In the third phase, twelve (12) scenarios of scavenging designs for the next 50 years were developed. It was found that using total extraction rates between 0.5 mgd and 1 mgd (million gallons per day) would effectively reduce the chloride concentration at EB-658. Similar concentration reduction at EB-658 was found using two different initial chloride concentrations (5,500 mg/L and 10,000 mg/L) in the southern area of the Baton Rouge fault. Using the optimization technique, the project found scenarios to have equal performance for chloride concentration reduction at EB-658, given the same total extraction rates. Using 1 mgd extraction rate, chloride concentration at EB-658 would reduce to the baseline chloride concentration in 20 years. However, pressure difference across the Baton Rouge fault would increase 1.8 m or less. Nevertheless, the increase is insignificant in comparison with the magnitude of current pressure difference.

1. Introduction

The goal of the project is to develop a **s**cavenger **w**ell **op**eration (SWOP) model to assist the Baton Rouge Water Company (BRWC) to cost-effectively stop saltwater intrusion toward the BRWC water wells at Lula pump station in the "1,500-foot" sand of the Baton Rouge area. On October 28, 2009, chloride concentration of 182 mg/L was measured at the water well EB-658 (Lula-19). This poses a concern that a high chloride front may have come near the Lula wells. To better understand the current situation of saltwater intrusion and to resolve this urgent issue, the SWOP model specifically aims to utilize scavenger wells to prevent high chloride concentration from reaching EB-658. Scavenger wells are small extraction wells to be placed at a certain distance in front of water wells to capture saltwater. The decision variables in the SWOP model are the number, location, and extraction rate of scavenger wells. The project consists of three major tasks to achieve the goal:

Task 1:   Develop and calibrate a "1,500-foot" sand saltwater intrusion model.
Task 2:   Evaluate saltwater intrusion for the next 50 years under current pumpage rate.
Task 3:   Develop scavenging designs to reduce chloride concentrations at EB-658.

Specific objectives are to:
(1) Understand the past, current, and future saltwater intrusion patterns
(2) Estimate the flux of groundwater flow across the Baton Rouge fault
(3) Estimate the flux of chloride concentration across the Baton Rouge fault
(4) Determine the number, location, and extraction rate of scavenger wells that can effectively stop saltwater intrusion to EB-658
(5) Evaluate the impact of scavenger wells on increasing saltwater intrusion across the fault

The entire modeling period was divided into a model calibration period and a model prediction period. Model calibration period was from 1/1/1945 to 12/31/2009, a 65-year period. In the calibration period, groundwater head data and chloride data were used to estimate model parameters. Simulated groundwater head and chloride concentration distributions at the end of 12/31/2009 were used as initial conditions (beginning of 1/1/2010) for the model prediction period. Model prediction period was a 50-year period from 1/1/2010 to 12/31/2059. Twelve (12) scenarios of scavenger well operations were tested in the model prediction period.

In the report, modeling results at the beginnings of three specific dates (1/1/2010, 1/1/2035, and 1/1/2060) were particularly discussed. These three dates served as the check points to evaluate groundwater heads and chloride concentrations at the current situation and situations after 25 and 50 years. It is noted that the information at the beginning of 1/1/2010 was that at the end of 12/31/2009, the information at the beginning of 1/1/2035 was that at the end of 12/31/2034, and the information at the beginning of 1/1/2060 was that at the end of 12/31/2059.

2. Saltwater intrusion model development

The "1,500-foot" sand saltwater intrusion model was developed using MODFLOW (Harbaugh et al., 2000) and MT3DMS (Zheng and Wang, 1999) under Groundwater Modeling System (GMS) (AQUAVEO[TM]). The terrain of the study area is shown in Figure 1, which covers the Baton Rouge metropolitan area. The eastern boundary of the study area extended to the Amite River, the western boundary was along the Mississippi River, the northern boundary intersected the north end of I-110 freeway, and the southern boundary was around 600 meters south of the Baton Rouge fault. It covered an area of around 300 km^2. The area was discretized into 188 rows, 195 columns, and 1 layer. The modeling area and computational grid are shown in Figure 2. Coarse computational cells of 200 m by 200 m were given at the northeastern area, where saltwater intrusion was not a concern. Finer computational cells of around 50 m by 50 m were given to the area of ongoing saltwater intrusion. Table 1 lists spatial and temporal discretizations for MODFLOW and MT3DMS models. The aquifer thickness was determined from the prior studies (Tsai and Li, 2008; Li and Tsai, 2009).

It was understood that saltwater intrusion is a density-dependent flow process. Flow process should be coupled with mass transport process at each time step to reveal encroachment of denser saltwater near the bottom of an aquifer. Since this modeling study served for the planning purpose and only considered one vertical layer to the "1,500-foot" sand in order to reduce computation complexity, density effect was not simulated. This means that MODFLOW and MT3DMS were decoupled. MODFLOW was run first to obtain groundwater levels. Then, MT3DMS was run using MODFLOW solutions to simulate intrusion of chloride concentration. In the future work, density effect can be simulated by discretizing the aquifer thickness into multiple layers.

In order to better predict the history of saltwater intrusion in the "1,500-foot" sand, the starting date of modeling was 1/1/1945. This was determined according to the timeline of installation of the BRWC water wells in the "1,500-foot" sand as shown in Figure 3. The first BRWC water well EB-413 was installed in 1946 at the Government pump station. From USGS studies (Meyer and Turcan, 1955), saltwater intrusion in the study area was not reported prior to 1946. In this study, the period prior to 1946 is denoted as the pre-anthropogenic pumping period.

2.1 Groundwater head initial condition on 1/1/1945

Groundwater head data for a 65-year calibration period 1/1/1945-12/31/2009 was collected from the USGS National Water Information System (NWIS), Groundwater Levels for Louisiana. In 1944-1945 groundwater level data at EB-84, 89, 94, 101, 157, 305, 310, 311, 312, and 448 showed similar groundwater level in the "1,500-foot" sand north of the Baton Rouge fault before significant anthropogenic withdrawals. The water level on 1/1/1945 was estimated at 19.5 m above mean sea level (msl). All groundwater heads in the report are with respect to the msl. Groundwater head data in the "1,200-foot" sand south of the fault was very limited. There was no direct head data for the early 1940s. EB-326 indicated water level of 19.51 m (64 feet) above msl in October 1936 in the "1,200-foot" sand south of the fault. Head data at EB-84, 89, 311, and 312 were used to estimated water level in October 1936 in the "1,500-foot" sand north of the fault, and found it to be 22.86 m (75 feet) above msl. This implies that during pre-anthropogenic

pumping groundwater level in the "1,500-foot" sand north of the fault was higher than groundwater level in the "1,200-foot" sand south of the fault. Fresh groundwater north of the fault might flow southward across the fault into the saltwater aquifer and create freshwater lenses south of the fault.

In the study area, groundwater level in the "1,200-foot" sand south of the fault was spatially similar due to low fault permeability to the horizontal flow. Therefore, it may be thought that water level in October 1936 at EB-326 was similar to that at EB-219 and EB-780A in the "1,200-foot" sand south of the fault. Using head data at EB-291 and EB-780A, groundwater level on 1/1/1945 was then estimated to be 16.7 m above msl.

2.2 Groundwater head boundary condition for 1/1/1945-12/31/2009

A time-varied head boundary condition was assigned to all boundary cells in MODFLOW. The south boundary head values were determined by the head data at EB-780A. Linear interpolation on EB-780A data was used to fill head values to the dates without measurements. The south boundary cells were assigned the same groundwater level at a given time, but different head values were used at different times. Groundwater head values along the boundary cells in the "1,500-foot" sand were carefully determined according to head observation data.

2.3 Chloride concentration initial condition on 1/1/1945

Zero chloride concentration was assigned throughout the entire "1,500-foot" sand. Chloride data was very limited in the "1,200-foot" sand. EB-198C showed 1,500 mg/L in 1936, but no chloride measurements after. However, measured chloride data at EB-219 and EB-326 only showed tens mg/L in 1963, and EB-782B showed 930 mg/L in 2003. No chloride data higher than 10,000 mg/L was reported in the "1,200-foot" sand south of the fault. The maximum chloride concentration at EB-780A was observed at 3,800 mg/L on December 1996. Based on many trials and errors and limited to moderate chloride concentration data, the initial concentration was assigned to be 5,500 mg/L in the "1,200-foot" sand. Moreover, a freshwater lens of 150 m wide south of the fault was assumed to reflect the southward freshwater flow across the fault in the pre-anthropogenic pumping period.

Some inconsistency on the trend of chloride concentration in the "1,500-foot" sand was observed. If saltwater encroachment was straight from EB-782B toward the Lula wells, then logically, chloride concentrations at EB-782B should always be higher than those at EB-807A. This trend was right before 1979. However, after 1979, chloride concentrations at EB-782B remained relatively low (less than 900 mg/L) while chloride concentrations at EB-807A were skyrocketing to 3,800 mg/L in December 1996. If chloride data at EB-807A is right, then chloride data at EB-782B after 1979 may not be correct.

2.4 Chloride concentration boundary condition for 1/1/1945-12/31/2009

Constant chloride concentration of 5,500 mg/L was assigned to the south boundary cells. Zero concentration gradient was assigned to all other boundary cells.

2.5 Water wells

Sixteen (16) water wells were installed in the study area during the period 1/1/1945-12/31/2009. Pumpage data was obtained from the Capital Area Ground Water Conservation Commission (CAGWCC) and BRWC. EB-504 was a BRWC water well, which was completed in 1949 and was out of service in 1979. EB-1295C (Stumberg-02) screened both the "1,500-foot" and "1,700-foot" sands. CAGWCC assigned EB-1295C pumpage record to the "1,500-foot" sand. This study included EB-1295C water well.

There was no pumpage data for EB-371B and EB-773 prior to 1975. EB-371B was completed in 1941 (Meyer and Turcan, 1955). Monthly pumpages for 1945-1974 at EB-371B and for 1964-1974 at EB-773 were determined by their 5-year monthly pumpage averages (1975-1979).

BRWC had lump sum pumpage data at water wells EB-413 and EB-504 for 1953-1962. To split EB-413 from EB-504 for this period, weighting coefficients for EB-413 were determined using the ratios of three-year monthly pumpage averages (1975-1977) to lump sum pumpages: EB-413 pumpages/(EB-413+EB-504 pumpages). BRWC also had lump sum pumpage data of water wells EB-413, EB-504, and EB-771 for 1963-1974. The same approach of deriving weighting coefficients was applied to splitting the lump sum pumpages for this period.

BRWC had lump sum pumpage data of water wells EB-510, EB-657, EB-658, EB-726, EB-938, and EB-939 for 1953-1974. For splitting the pumpages, weighting coefficients were obtained using the ratios of five-year monthly averages (1975-1979) of their individual pumpages to the lump sum pumpages in this 5-year period.

Finally, the monthly pumpages for 1946-1952 at EB-413 were determined by 5-year monthly pumpage averages (1953-1957). The monthly pumpages for 1949-1952 at EB-504 were determined by 5-year monthly pumpage averages (1953-1957).

The "Connector" Well

The connector well, EB-1293, started in April 1999. Since the recorded groundwater data at EB-1293 did not represent head in the "1,500-foot" sand, the head data could not be used to assign a constant head boundary condition, or could not be used to compare to simulated water levels at EB-1293. Instead, recorded flow rate was used to represent EB-1293 as an injection well in the model. According to January 2009 CAGWCC Newsletter, the average injection rate was 475 gallons per minute or 2,589 m^3/day (or 0.684 mgd).

3. Calibration results

3.1 Groundwater flow model

Table 2 shows the estimated MODFLOW parameter values. Homogeneous hydraulic conductivity of 55 m/day was used in the groundwater model. A homogeneous fault hydraulic characteristic (fault hydraulic conductivity per unit fault width) (Hsieh and Freckleton, 1993) was estimated 8.0×10^{-4} day^{-1} for a segment from the west boundary to the intersection of Wards Creek and Corporate Boulevard. The other segment of the fault had a relatively low hydraulic characteristic value of 3.5×10^{-4} day^{-1}. As shown in Figure 4, simulated groundwater levels compare well to the observed data for different time periods at several observation wells. According to water level in EB-917, groundwater level declined at a rate of 1.31 m/year (4.3 ft/year) before 1980, 0.40 m/year (1.3 ft/year) in the 1980s and 1990s, and 1.16 m/year (3.8 ft/year) after 2000. Figure 5 shows the simulated groundwater distribution at the beginning of 1/1/2010. A cone of depression centered at Lula pump station is evident.

Pore water pressure differences and groundwater flow velocity (Darcy velocity) across the Baton Rouge fault were estimated at a single point using simulated groundwater heads at EB-782B and at its adjacent computational cell (134, 71) south of the fault. Using the harmonic mean approach, equivalent hydraulic conductivity for this calculation was obtained 0.081 m/day. The results are shown in Figure 6. Negative water pressure difference and negative flow velocity occurred at the beginning of a few years of simulation because of southward flow across the fault. Figure 6 shows a trend of increasing pressure difference and flow velocity in the last 10 years (2000-2009). Pressure difference on 1/1/2010 was estimated at 43 psi (pounds per square inch). The flow velocity was estimated at 4.84×10^{-2} m/day on 1/1/2010.

The maximum head pressure difference on 1/1/2010 occurred around 100 m west of the intersection of Dalrymple Drive and the fault line. The computational cell (137, 39) south of the fault had groundwater head of -7.957 m and the computational cell (136, 39) north of the fault had groundwater head -38.852 m. This resulted in head difference 44 psi and flow velocity 4.94×10^{-2} m/day on 1/1/2010. The maximum pressure difference was only one psi higher than that at EB-728B.

3.2 Chloride transport model

Table 3 shows the estimated MT3DMS parameter values. Porosity was estimated 27%, longitudinal dispersivity was estimated 180 m, and transverse dispersivity was estimated 0.36 m. The same homogeneous porosity, longitudinal dispersivity, and transverse dispersivity were used for both "1,200-foot" sand and "1,500-foot" sand. It was observed that major chloride concentration at EB-917 and EB-918 might be the result of lateral-flow-driven chloride transport along the fault from the east side. Therefore, a high ratio of longitudinal dispersivity to transverse dispersivity was obtained to reveal faster chloride transport to EB-807A and EB-658, but slower chloride transport to EB-917 and EB-918.

Simulated chloride breakthroughs were compared to chloride data shown in Figure 7. Simulated chloride concentrations showed up earlier compared to lower chloride data at EB-807A, but were similar to high chloride data. Simulated chloride concentrations showed good agreement to the chloride data at EB-807A after 1981, and to the chloride data at EB-917 and EB-658 after 2000. Simulated chloride concentrations were underestimated at EB-918 after 2000. This indicates that chloride transport simulation along the fault from the eastern side needs more study. However, the lateral-flow-driven chloride concentration showed less impact on EB-658 and EB-807A.

The 65-year simulation in Figure 8 shows a unique movement of the saltwater intrusion front. From 1945 to 1987, a single chloride front was developed and moved toward EB-771 (Government-06). From 1987 to 2001, the front started to retreat and a new front started to develop and move toward the Lula wells. From 2001 to 2009, a single front moved toward EB-658 (Lula-19). Chloride concentration distribution on 1/1/2010 is shown in Figure 9. This unique movement of chloride concentrations was revealed by the "up-down-up" chloride data at EB-917. The unique intrusion pattern is the combined effect of the low permeable Baton Rouge fault and dynamic anthropogenic pumping.

Chloride mass flux was estimated at a single point using simulated groundwater flow velocity in Figure 6 and simulated chloride concentrations at EB-782B and its adjacent computational cell (134, 71) north of the fault. Advective mass flux (kg/day-m^2), dispersive mass flux, and total mass flux (advective+dispersive mass fluxes) of chloride are shown in Figure 10. The magnitudes of advective mass flux and dispersive mass flux were similar prior to 1957. After 1957, advective mass flux dominated dispersive mass flux due to high groundwater flow velocity. Dispersive mass flux was strong in 1955-1980. The total mass flux on 1/1/2010 was estimated 0.98 kg/day-m^2.

4. Saltwater intrusion prediction

4.1 The no-action scenario (no scavenger wells)

The saltwater intrusion model was run for 50 years from 1/1/2010 to 12/31/2059 without scavenger wells. Predicted breakthrough curves in EB-658 and other observation wells were used as baseline information to evaluate the stopping efficiency of various scenarios through using scavenger wells as presented in the following section.

To extend the saltwater intrusion model to predict chloride concentrations in the period 1/1/2010-12/31/2059, time-varied boundary values of groundwater head were estimated using the linear trend of head declination in the last 5 years, 1/1/2005-12/31/2009. The monthly pumpages of water wells were estimated based on 5-year (2005-2009) averaged pumpages. Table 4 lists the monthly pumpages used for the prediction period. The total withdrawal rate at Government pump station (two water wells) was 2.53 mgd, at Lula pump station (six water wells) was 7.07 mgd, and at N. 45th pump station (one water well) was 1.69 mgd. The total pumpage of water wells in Table 4 was 12.45 mgd. The injection rate of the connector well remains 0.684 mgd, and chloride concentration at the southern boundary remains 5,500 mg/L throughout the prediction period.

Figure 11 shows increasing chloride concentrations at EB-658, EB-807A, EB-917, and EB-918 in the period 1/1/1945-12/31/2059. Chloride concentration in EB-658 was predicted to 754 mg/L on 1/1/2035 and 1,540 mg/L on 1/1/2060. Figure 12 shows the concentration distributions on 1/1/2035 and 1/1/2060. Table 5 lists predicted chloride concentrations at observation wells, Government wells, and the connector well on 1/1/2035 and 1/1/2060. Chloride concentrations in EB-807A, EB-917, and EB-918 were predicted to be thousands mg/L on 1/1/2035 and almost reach the maximum concentration 5,500 mg/L on 1/1/2060. Chloride concentrations in EB-413, EB-771, and EB-1293 were predicted tens mg/L on 1/1/2035, but would reach hundreds mg/L on 1/1/2060. Estimated chloride concentrations at N. 45th well, EB-927, were very low throughout the prediction period.

4.2 Scenarios of stopping saltwater intrusion to EB-658 using scavenger wells

The goal of using scavenger wells in this study is to protect EB-658 from high chloride concentration. Twelve (12) scenarios listed in Table 6 were designed for this goal. The starting date of using scavenger wells was assigned to 1/1/2011. The first four scenarios used one scavenger well with a constant extraction rate throughout the prediction period 1/1/2010-12/31/2059. Extraction rates with a 0.25 mgd increment increase were tested from 0.25 mgd to 1.00 mgd in scenario 1 to scenario 4, respectively. Scenarios 5-7 and scenario 9 used two concurrent scavenger wells, scenario 8 used three concurrent scavenger wells, and scenario 10 used four concurrent scavenger wells. Concurrent scavenger wells mean that scavenger wells were active from the beginning to the end of the prediction period.

Scenarios 11 and 12 considered two sequential scavenger wells. The first scavenger well was active with an extraction rate of 0.50 mgd entirely throughout the prediction period. However, the second scavenger well was only active between 1/1/2036 and 12/31/2059.

To reduce computation time, scenarios 5 and 6 adopted the scavenger well location in scenario 1 as their first scavenger well. Then, location of the second scavenger well was systematically searched. In the same manner, Scenario 8 was developed based on upon scenario 5, scenario 10 was developed based upon scenario 8, and scenarios 7, 9, 11, and 12 were developed based upon scenario 2. Using this stepwise approach, each scenario only searched for one scavenger well location at a time. Figure 13 shows the scenario map that correlates the hierarchical relationship and extraction rates among different scenarios.

A total of 36 potential locations of scavenger wells, named from SW1 to SW36, were predetermined in Figure 14. A new observation well, EB-xxxx (N 30' 27.285, W 91' 09.509) between SW13 and SW14 is currently being drilled by Layne at the time of the report preparation. It can be converted to a scavenger well if the SWOP model selects SW13 and/or SW14.

Scenarios 1 to 4 tested each potential location, and the chloride concentrations at EB-658 are shown in Figure 15. The numbers in Figure 15 are listed in Table 7. The best scavenger well location for scenario 1 was at SW21, which resulted in 385 mg/L on 1/1/2035 and 903 mg/L on 1/1/2060. It was obvious that scenario 1 was not a feasible solution. Scenario 2 was a feasible solution to keep chloride concentration less than 150 mg/L up to 1/1/2036. After that, the concentration started to rise up to 412 mg/L on 1/1/2060. Scenarios 3 and 4 were feasible solutions to keep low chloride concentration at EB-658. The best location of scavenger wells and the reduced chloride concentrations at EB-658 for scenarios 1-4 is listed in Table 8. Analysis from the solutions of first four scenarios is summarized below:

(1) If scavenger wells were placed too close to the Lula wells, high chloride concentration would be dragged near the Lula wells. EB-658 would pump high chloride concentration in later time.

(2) If scavenger wells were placed far away from the Lula wells in a high chloride concentration zone, high chloride concentrations north of the scavenger well could not be caught. High chloride concentrations would eventually arrive at EB-658.

(3) Scavenger wells had a tendency to locate at the first three columns since the chloride concentration was slowly leaning to the west due to the impermeable zone at the west side.

(4) Using high extraction rate, there were many feasible locations to install scavenger wells, in addition to the best location. Scavenger wells at the best location give the lowest concentration at EB-658.

Figure 16 shows the chloride concentrations at EB-658 for different potential locations of the last scavenger well in scenarios 5-12. Most of the scenarios limited the location search to the first three columns. The numbers in Figure 16 are listed in Table 9. Similarly, when extraction rate is high, many locations were feasible to install scavenger wells. The best locations of scavenger wells in the searching order and the simulated chloride concentrations in EB-658 on 1/1/2035

and 1/1/2060 are listed in Table 8. Scenario 5 was not a feasible solution for the period 1/1/2036-1/1/2060. Scenarios 6-12 were all feasible solutions to keep low chloride concentrations at EB-658 throughout the entire prediction period.

As shown in Figure 17, it was found that breakthrough curves at EB-658 using one single scavenger well and using multiple scavenger wells were similar for the same total extraction rates. For example, scenarios 3, 6, 7, and 8 used a total of 0.75 mgd, but different numbers of scavenger wells. The breakthrough curves were similar. Scenarios 4, 9, and 10 used a total of 1.00 mgd, but different numbers of scavenger wells. The breakthrough curves were similar. This result provides many options with the same total extraction rates.

All 12 scenarios showed little impact on chloride concentrations at EB-807A, EB-917, and EB-918, as shown in Figure 18. Scenario 10 showed the highest impact on those observation wells. Using scavenger wells may have a positive impact on reducing the chloride concentrations at Government wells and the connector well by dragging concentration to the west, as shown in Figure 19.

The impact of scenario 10 on the groundwater flow across the fault at EB-782B is shown in Figure 20. Without scavengers, the pressure difference linearly increased from 43 psi on 1/1/2010 to 82 psi on 1/1/2060. The groundwater flow linearly increased from 4.84×10^{-2} m/ day on 1/1/2010 to 9.19×10^{-2} m/day on 1/1/2060. As shown in Figure 21, the total mass flux increased from 0.98 kg/day-m^2 on 1/1/2010 to 1.87 kg/day-m^2 on 1/1/2060. Those values showed a 90% increase in 2060 with respect to the values on 1/1/2010. As shown in Figures 22 and 23, scenario 10 keeps the 250 mg/L front line away from the Lula wells for the next 50 years. However, the water wells at Government pump station would encounter high chloride concentration in 50 years. Using scenario 10, a total of one-mgd extraction rate caused additional drawdown of 0.02 m south of the fault and additional drawdown of 1.66 m north of the fault compared to the no-action scenario. This resulted in an additional 2.33 psi pressure difference and 2.62×10^{-3} m/day groundwater flow velocity. The total mass flux increased by 0.051 kg/day-m^2. Those values counted for less than 6% increase with respect to the values on 1/1/2010.

To better illustrate the performance of the 1-mgd scenarios, extra drawdowns created by scenarios 4, 9, and 10, with respect to the groundwater level on 1/1/2035 and 1/1/2060, for the no-action scenario are shown in Figures 24, 25 and 26, respectively. The extra drawdown distributions are static over the next 50 years. The scavenger wells have very little impact on reducing groundwater level south of the fault. The maximum extra drawdowns for scenarios 4, 9, and 10, are 2.72 m, 2.41 m and 2.27 m, respectively, and occur at the scavenger wells. Scenario 10 gives relative lower drawdown around the scavenger wells. Otherwise, these three scenarios would create similar drawdowns at relative remote areas.

5. High chloride concentration south of the fault

There is a concern that chloride concentration south of the Baton Rouge fault could be much higher than 5,500 mg/L since high chloride level was observed at other sands. For conservative scavenging designs, this section discussed the solutions of prior scenarios under initial concentration of 10,000 mg/L with a focus on scenarios 4, 9 and 10 (1 mgd extraction rate). The constant concentration at the southern boundary is also 10,000 mg/L.

Following the model calibration procedure, hydraulic characteristic for the Baton Rouge fault was reduced from 8.0×10^{-4} day^{-1} to 5.19×10^{-4} day^{-1}, porosity was estimated at 0.26, longitudinal dispersivity was estimated at 210 m, and transverse dispersivity was estimated at 2.47 m. The flow and transport model parameters are listed at Table 10. Calculated water levels as shown in Figure 27 compare well to the observed water levels at EB-782B, EB-917, EB-918, and EB-807A. Figure 28 shows the calculated chloride concentrations against the observed at EB-658, EB-917, EB-918 and EB-807A. Simulated chloride concentration was overestimated at EB-807A. This indicates that the predicted chloride concentration at the area between EB-807A and the Baton Rouge fault may be a bit higher than actual concentration. Therefore, if the suggested scavenging scenarios meet the saltwater stopping requirement under this condition, they would also be feasible for lower concentration.

Table 11 lists predicted chloride concentrations at observation wells, Government wells, and the connector well on 1/1/2035 and 1/1/2060 under the no-action scenario. Chloride concentrations in EB-807A, EB-917, and EB-918 were predicted to be thousands mg/L on 1/1/2035 and almost reach the maximum concentration 10,000 mg/L on 1/1/2060. Chloride concentrations in EB-413, EB-771, and EB-1293 were predicted tens mg/L on 1/1/2035, but would reach hundreds mg/L on 1/1/2060. The estimated chloride concentrations at N. 45th well, EB-927, were very low throughout the prediction period.

Table 12 lists chloride concentration at EB-658 on 1/12035 and 1/1/2060 for scenarios 1-12 against the no-action scenario. The lower values of chloride concentration in Table 12, with respect to Table 8, are due to higher longitudinal dispersivity for this case. It is interpreted that the reduction performance is literally the same as in Table 8. Again, using scenarios with total extraction rate 0.5 mgd or above would significantly reduce the chloride concentration at EB-658 for next 50 years. Using one-mgd extraction rate would reduce the concentration to baseline chloride concentration at EB-658. Chloride concentration at EB-658 for next 50 years under these scenarios is shown in Figure 29, which is similar to Figure 17. Therefore, scenarios 4, 9 and 10, if selected, would work for a concentration 10,000 mg/L or lower in the south of the Baton Rouge fault. The progress of stopping saltwater toward the Lula wells under scenario 10 is shown in Figures 30, 31 and 32. Scenario 10 would effectively keep the 250 mg/L front line away from the water wells at Lula pump station.

Figures 33, 34, and 35 show the extra drawdowns created by scenarios 4, 9, and 10 with respect to the groundwater level of the no-action scenario. The maximum extra drawdowns for scenario 4, 9, and 10 are 2.74 m, 2.42 m, and 2.29 m, respectively, and occur at location of scavenger wells. Again, scenario 10 gives relative lower drawdown around the scavenger wells.

16

Although not shown in the report, the intrusion pattern observed in Figure 8 was not changed for different chloride concentration south of the fault. Reduction of chloride concentration at EB-413, EB-771 and EB-1293 and increase of chloride concentration at EB-807A, EB-917 and EB-918 also was observed for this case.

6. Conclusions

[1] The simulation results of using chloride concentration 5,000 mg/L and 10,000 mg/L in the southern area of the Baton Rouge fault predicted similar chloride concentration at EB-658 for next 50 years. At 5-year averaged withdrawal rates (2005-2009), EB-658 would encounter high chloride concentration, around 750 mg/L within the next 25 years and around 1,500 mg/L within the next 50 years.

[2] Using scavenger wells with a total of extraction rates less than or equal to 1 mgd is possible to keep chloride concentrations at EB-658 lower than 150 mg/L in next 50 years. Using 1-mgd extraction rate would reduce concentration to baseline chloride concentration at EB-658.

[3] Stopping performance using multiple wells is similar to using a single well for the same total extraction rates.

[4] Using high extraction rates, many feasible locations are available, in additional to the best location, for installing scavenger wells.

[5] Scavenger wells may increase chloride concentrations at EB-807A, EB-917 and EB-918.

[6] Scavenger wells may effectively reduce chloride concentrations at Government wells (EB-413 and EB-771) and at the connector well (EB-1293).

[7] Using a total extraction rate less than 1 mgd, scavenger wells may induce extra drawdown less than 1.8 m to the northern area along the fault, but show very little or no impact to groundwater level south of the fault.

[8] Scavenger wells with extraction rates 1 mgd or less may increase pressure difference, flow velocity, and mass rate across the Baton Rouge fault by less than 6% with respect to the condition on 1/1/2010.

7. Recommendations

[1] Potential locations of scavenger wells are at SW13, SW19, SW20, and SW21.

[2] At least 0.50 mgd of a total extraction rate would be needed to reduce chloride concentrations at EB-658 to less than 150 mg/L for the next 25 years.

[3] All scenarios except scenarios 1, 2, and 5 are feasible solutions throughout 1/1/2060.

[4] Using scenario 5, the Lula wells would be fine up to 1/1/2035 (less than 150 mg/L). Either Scenario 11 or 12 may be considered after 1/1/2035.

[5] The use of multiple wells may be preferred in order to reduce drawdown around the scavenger wells. With this regard, scenario 8 is recommended for 0.75 mgd, and scenario 10 is recommended for 1.00 mgd.

[6] The new observation well, EB-xxxx, which is very close to SW13, is recommended to be converted to a scavenger well for scenarios 4, 6, and 8-12.

References

Harbaugh, A. W., E. R. Banta, M. C. Hill, and M. G. McDonald. (2000). MODFLOW-2000, the U.S. Geological Survey modular ground-water model: User guide to modularization concepts and the ground-water flow process. U.S. Geological Survey Open-File Report 00-92.

Hsieh, P. A., and J. R. Freckleton. (1993). Documentation of a computer program to simulate horizontal-flow barriers using the U.S. Geological Survey modular three- dimensional finite-difference ground-water flow model: U.S. Geological Survey Open-File Report 92-477, 32 p.

Li, X., and F. T.-C. Tsai. (2009). Bayesian model averaging for groundwater head prediction and uncertainty analysis using multimodel and multimethod. Water Resources Research, 45, W09403, doi:10.1029/2008WR007488.

Meyer, R. R., and A. N. Turcan, Jr. (1955). Geology and Ground Water Resources of the Baton Rouge Area, Louisiana, Louisiana: U. S. Geological Survey Water-Supply Paper 1296, 138p.

Rollo, J. R. (1969). Saltwater encroachment in aquifers of the Baton Rouge area, Louisiana: Department of Conservation, Louisiana Geological Survey, and Louisiana Department of Public Works Water Resources Bulletin no. 13, 45 p.

Tsai, F. T.-C., and X. Li. (2008). Inverse groundwater modeling for hydraulic conductivity estimation using Bayesian model averaging and variance window. Water Resources Research 44(9), W09434, doi:10.1029/2007WR006576.

Zheng, C., and P. Wang. (1999). MT3DMS, A modular three-dimensional multispecies transport model for simulation of advection, dispersion and chemical reactions of contaminants in groundwater systems (Release DoD_3.50.A), Documentation and User's Guide.

Tables

Table 1: Spatial and temporal discretizations in MODFLOW and MT3DMS.

Parameter	Value
Number of layers	1
Number of rows	188
Number of columns	195
Length of stress periods	month
Number of stress periods for model calibration	780
Number of stress periods for model prediction	600
Time unit	day
Length unit	m

Table 2: Estimated flow parameter values in MODFLOW.

Parameter	Value	Unit
Hydraulic conductivity for the "1,500-foot" sand and the "1,200-foot" sand	55.0	m/day
Specific storage	2.2104×10^{-5}	m^{-1}
Hydraulic characteristic (Hsieh and Freckleton, 1993) for the Baton Rouge fault from the west boundary to the intersection of Wards Creek and Corporate Blvd	8.0×10^{-4}	day^{-1}
Hydraulic characteristic for the rest of the fault line	3.5×10^{-4}	day^{-1}
Initial head (01/01/1945) north of the fault	19.5	m
Initial head (01/01/1945) south of the fault	16.7	m

Table 3: Estimated mass transport parameter values in MT3DMS.

Parameter	Value	Unit
Initial concentration (01/01/1945) south of the fault	5500	mg/L
Initial concentration (01/01/1945) north of the fault	0	mg/L
Constant concentration at southern boundary	5500	mg/L
Porosity	0.27	-
Longitudinal dispersivity	180	m
Transverse dispersivity	0.36	m

Table 4: Five-year average (2005-2009) withdrawal rates of water wells for the prediction period 1/1/2010-1/1/2060.

USGS well name	Local name	5-year average withdrawal rate (m^3/day)	5-year average withdrawal rate (mgd)
EB-371B	DSM	0	0
EB-413	Government-03	5440.6	1.437
EB-504	Government-04	0	0
EB-510	Lula-17	5644.0	1.491
EB-657	Lula-18	993.9	0.263
EB-658	Lula-19	4793.6	1.266
EB-726	Lula-20	5989.9	1.583
EB-771	Government-06	4137.4	1.093
EB-773	Robin-01	1789.6	0.473
EB-905	Parish Water	0	0
EB-927	N. 45th-03	6403.9	1.692
EB-938	Lula-22	5146.0	1.360
EB-939	Lula-23	4178.9	1.104
EB-961	Cortana-05	801.1	0.212
EB-996	BRWC	0	0
EB-1295C	Stumberg-02	1787.3	0.472
EB-1293	Connector Well	-2589.0	-0.684

Table 5: Predicted chloride concentrations with no scavenger wells (the no-action scenario).

Well name	Concentration (mg/L)	
	1/1/2035	1/1/2060
EB-658	754	1540
EB-413	9	361
EB-771	57	430
EB-807A	5454	5493
EB-917	2845	5307
EB-918	4008	5404
EB-1293	11	170

Table 6: Scenarios of scavenger well operation.

Scenario	Scavenger well operation (SWOP)
1	One scavenger well with 0.25 mgd
2	One scavenger well with 0.50 mgd
3	One scavenger well with 0.75 mgd
4	One scavenger well with 1.00 mgd
5	Two concurrent scavenger wells: the 1st well with 0.25 mgd and the 2nd well with 0.25 mgd
6	Two concurrent scavenger wells: the 1st well with 0.25 mgd and the 2nd well with 0.50 mgd
7	Two concurrent scavenger wells: the 1st well with 0.50 mgd and the 2nd well with 0.25 mgd
8	Three concurrent scavenger wells: the 1st well with 0.25 mgd, the 2nd well with 0.25 mgd, and the 3rd well with 0.25 mgd
9	Two concurrent scavenger wells: the 1st well with 0.50 mgd and the 2nd well with 0.50 mgd
10	Four concurrent scavenger wells: the 1st well with 0.25 mgd, the 2nd well with 0.25 mgd, the 3rd well with 0.25 mgd, and the 4th well with 0.25 mgd
11	Two sequential scavenger wells: the 1st well with 0.50 mgd and the 2nd well with 0.25 mgd
12	Two sequential scavenger wells: the 1st well with 0.50 mgd and the 2nd well with 0.50 mgd

Table 7: Simulated chloride concentrations (mg/L) at EB-658 on 1/1/2035 and 1/1/2060 using one scavenger well with four different extraction rates at 36 possible locations, scenarios 1 to 4.

Well name	UTM-NAD83, x (meters)	UTM-NAD83, y (meters)	Scenario 1 0.25 MGD		Scenario 2 0.5 MGD		Scenario 3 0.75 MGD		Scenario 4 1.00 MGD	
			1/1/2035	1/1/2060	1/1/2035	1/1/2060	1/1/2035	1/1/2060	1/1/2035	1/1/2060
SW1	676779	3371121	544	1029	321	642	145	324	73	164
SW2	676829	3371121	465	945	227	517	97	239	52	124
SW3	676879	3371121	431	969	208	515	107	275	56	127
SW4	676926	3371121	489	1010	271	634	157	418	91	231
SW5	676976	3371121	577	1184	412	876	266	620	161	413
SW6	677029	3371121	707	1321	594	1140	432	914	306	671
SW7	676779	3370870	457	935	181	438	62	148	20	44
SW8	676829	3370870	397	898	167	443	60	168	20	49
SW9	676879	3370870	408	930	195	516	77	235	30	91
SW10	676926	3370870	448	989	246	608	127	344	55	171
SW11	676976	3370870	519	1073	347	764	213	528	102	307
SW12	677029	3370870	617	1229	464	952	324	749	183	494
SW13	676779	3370623	410	902	151	412	38	144	10	17
SW14	676829	3370623	398	890	147	430	40	146	11	29
SW15	676879	3370623	401	927	168	497	56	217	16	74
SW16	676926	3370623	439	986	211	563	92	295	31	126
SW17	676976	3370623	473	1021	275	661	148	409	59	204
SW18	677029	3370623	533	1963	353	810	208	547	101	325
SW19	676779	3370371	405	913	147	386	39	95	15	9
SW20	676829	3370371	392	910	143	412	40	122	14	20
SW21	676879	3370371	385	903	163	436	51	174	18	43
SW22	676926	3370371	401	921	179	491	74	225	26	77
SW23	676976	3370371	434	962	213	541	103	306	40	144
SW24	677029	3370371	464	969	265	649	144	407	63	202
SW25	676779	3370122	419	872	164	365	66	81	34	8.5
SW26	676829	3370122	398	902	162	369	62	96	33	13
SW27	676879	3370122	392	903	164	394	65	133	33	26
SW28	676926	3370122	403	914	181	431	83	167	39	47
SW29	676976	3370122	410	940	197	464	94	224	47	77
SW30	677029	3370122	424	946	222	518	118	278	62	119
SW31	676779	3369870	433	881	207	336	99	75	65	16
SW32	676829	3369870	433	866	200	342	101	83	61	18
SW33	676879	3369870	411	885	205	353	99	100	64	22
SW34	676926	3369870	421	883	206	372	105	121	66	31
SW35	676976	3369870	409	866	209	394	116	155	68	49
SW36	677029	3369870	441	917	225	431	137	208	78	76

Table 8: Simulated chloride concentrations at EB-658 using the best solutions in individual scenarios.

Scenario	Scavenger well	Concentration (mg/L)	
		1/1/2035	1/1/2060
No action	-	754	1540
1	SW21	385	903
2	SW20	143	412
3	SW20	40	122
4	SW13	10	17
5	SW21, SW19	147	399
6	SW21, SW13	35	114
7	SW20, SW19	39	115
8	SW21, SW19, SW13	33	110
9	SW20, SW13	9	15
10	SW21, SW19, SW13, SW7	7	16
11	SW20, SW13	143	116
12	SW20, SW13	143	19

Table 9: Location of the last scavenger well in scenarios 5 to 12 and simulated chloride concentrations (mg/L) at EB-658 on 1/1/2035 and 1/1/2060.

Well name	UTM-NAD83, x (meters)	UTM-NAD83, y (meters)	Scenario 5 0.25 mgd		Scenario 6 0.50 mgd		Scenario 7 0.25 mgd		Scenario 8 0.25 mgd		Scenario 9 0.50 mgd		Scenario 10 0.25 mgd		Scenario 11 0.25 mgd	Scenario 12 0.50 mgd
			1/1/2035	1/1/2060	1/1/2035	1/1/2060	1/1/2035	1/1/2060	1/1/2035	1/1/2060	1/1/2035	1/1/2060	1/1/2035	1/1/2060	1/1/2060	1/1/2060
SW1	676779	3371121	245	545	116	263	81	188	76	183	31	76	15	39	189	83
SW2	676829	3371121	187	493	76	208	52	156	52	157	21	70	9	31	160	67
SW3	676879	3371121	192	491	81	238	62	207	66	205	27	95	14	55	199	90
SW7	676779	3370870	165	436	48	141	42	122	43	120	13	34	7	16	128	32
SW8	676829	3370870	152	458	49	160	42	148	41	148	12	40	7	26	145	41
SW9	676879	3370870	174	515	70	244	55	210	56	211	18	80	10	50	203	77
SW13	676779	3370623	143	414	35	114	34	180	33	110	9	15	10	16	116	19
SW14	676829	3370623	154	437	43	155	37	141	36	135	10	28	10	19	138	32
SW15	676879	3370623	165	483	63	218	47	170	46	179	12	54	13	30	182	54
SW19	676779	3370371	147	399	41	110	39	115	41	180	15	13	9	12	130	31
SW20	676829	3370371	149	409	43	136	40	124	41	119	14	20	9	16	137	34
SW21	676879	3370371	161	439	51	175	43	136	45	132	16	30	9	17	149	34
SW25	676779	3370122	159	412	53	121	45	116	46	113	20	13	11	15	149	42
SW26	676829	3370122	156	428	55	140	47	120	46	116	20	17	11	15		47
SW27	676879	3370122	162	430	60	162	46	136	46	128	20	23	11	17		54
SW31	676779	3369870	175	420	71	134	50	121	52	116	25	17	12	15	165	59
SW32	676829	3369870	177	432	74	150	53	131	52	120	24	20	12	17		62
SW33	676879	3369870	178	443	76	158	53	130	54	123	25	24	12	16		67

Table 10: Estimated flow and transport parameter values in MODFLOW and MT3DMS, C_0=10,000 mg/L case.

Parameter	Value	Unit
Hydraulic conductivity for the "1,500-foot" sand and the "1,200-foot" sand	55.0	m/day
Specific storage	2.2104×10^{-5}	m^{-1}
Hydraulic characteristic (Hsieh and Freckleton, 1993) for the Baton Rouge fault from the west boundary to the intersection of Wards Creek and Corporate Blvd	5.19×10^{-4}	day^{-1}
Hydraulic characteristic for the rest of the fault line	3.5×10^{-4}	day^{-1}
Initial head (01/01/1945) north of the fault	19.5	m
Initial head (01/01/1945) south of the fault	16.7	m
Initial concentration (01/01/1945) south of the fault	10000	mg/L
Initial concentration (01/01/1945) north of the fault	0	mg/L
Constant concentration at southern boundary	10000	mg/L
Porosity	0.26	-
Longitudinal dispersivity	210	m
Transverse dispersivity	1.47	m

Table 11: Predicted chloride concentrations with no scavenger wells (the no-action scenario), C_0=10,000 mg/L case.

Well name	Concentration (mg/L)	
	1/1/2035	1/1/2060
EB-658	746	1498
EB-413	5	251
EB-771	32	350
EB-807A	9353	9904
EB-917	3001	8352
EB-918	6398	9596
EB-1293	5	161

Table 12: Simulated chloride concentrations at EB-658 under individual scenarios, C_0=10,000 mg/L case.

Scenario	Scavenger well	Concentration (mg/L)	
		1/1/2035	1/1/2060
No action	-	746	1498
1	SW21	366	851
2	SW20	107	303
3	SW20	28	73
4	SW13	16	20
5	SW21, SW19	107	303
6	SW21, SW13	26	70
7	SW20, SW19	26	57
8	SW21, SW19, SW13	21	54
9	SW20, SW13	12	18
10	SW21, SW19, SW13, SW7	4	12
11	SW20, SW13	107	60
12	SW20, SW13	107	17

Figures

Figure 1: The study area (the Baton Rouge area, Louisiana). All of the wells in the figure are screened at the "1,500-foot" sand. Layne is drilling a new observation well, EB-xxxx (N 30' 27.285, W 91' 09.509), around 900 m south of EB-658 at the time of the report preparation.
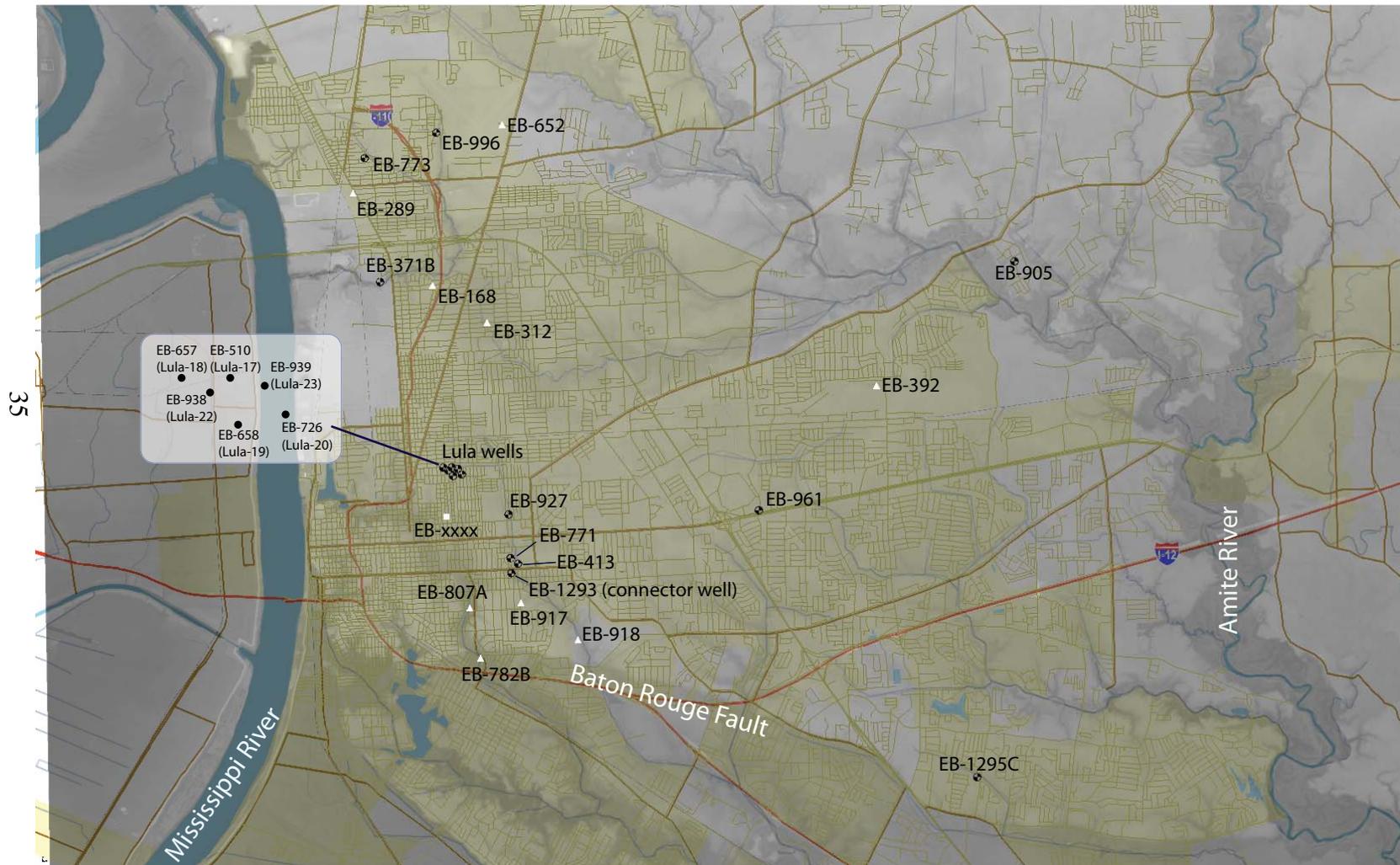
(Base Map and LIDAR DEM obtained from Atlas: The Louisiana Statewide GIS, http://atlas.lsu.edu/)

Figure 2: Spatial discretization of the study domain.
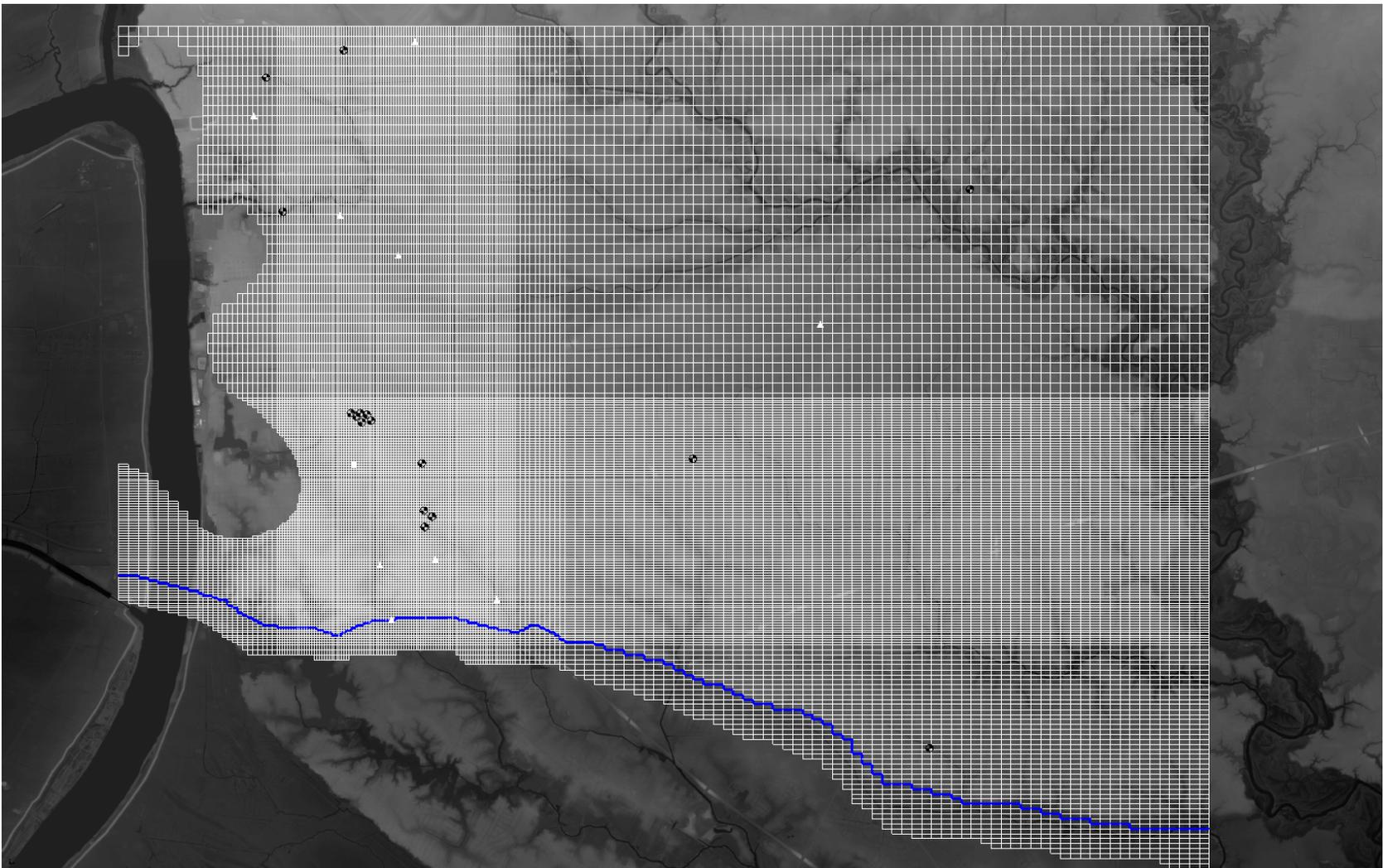
Figure 3: Timeline of the BRWC water wells in the "1,500-foot" sand.
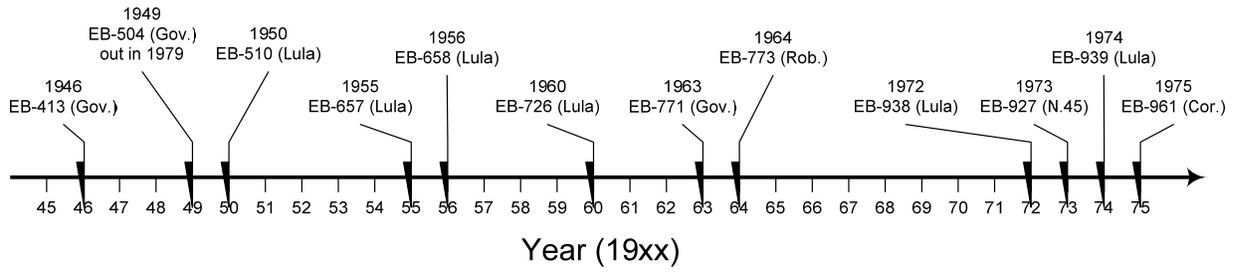
Figure 4: Calibration result of the MODFLOW model for the period 1/1/1945-12/31/2009. Lines represent simulated groundwater heads and filled circles represent head data.
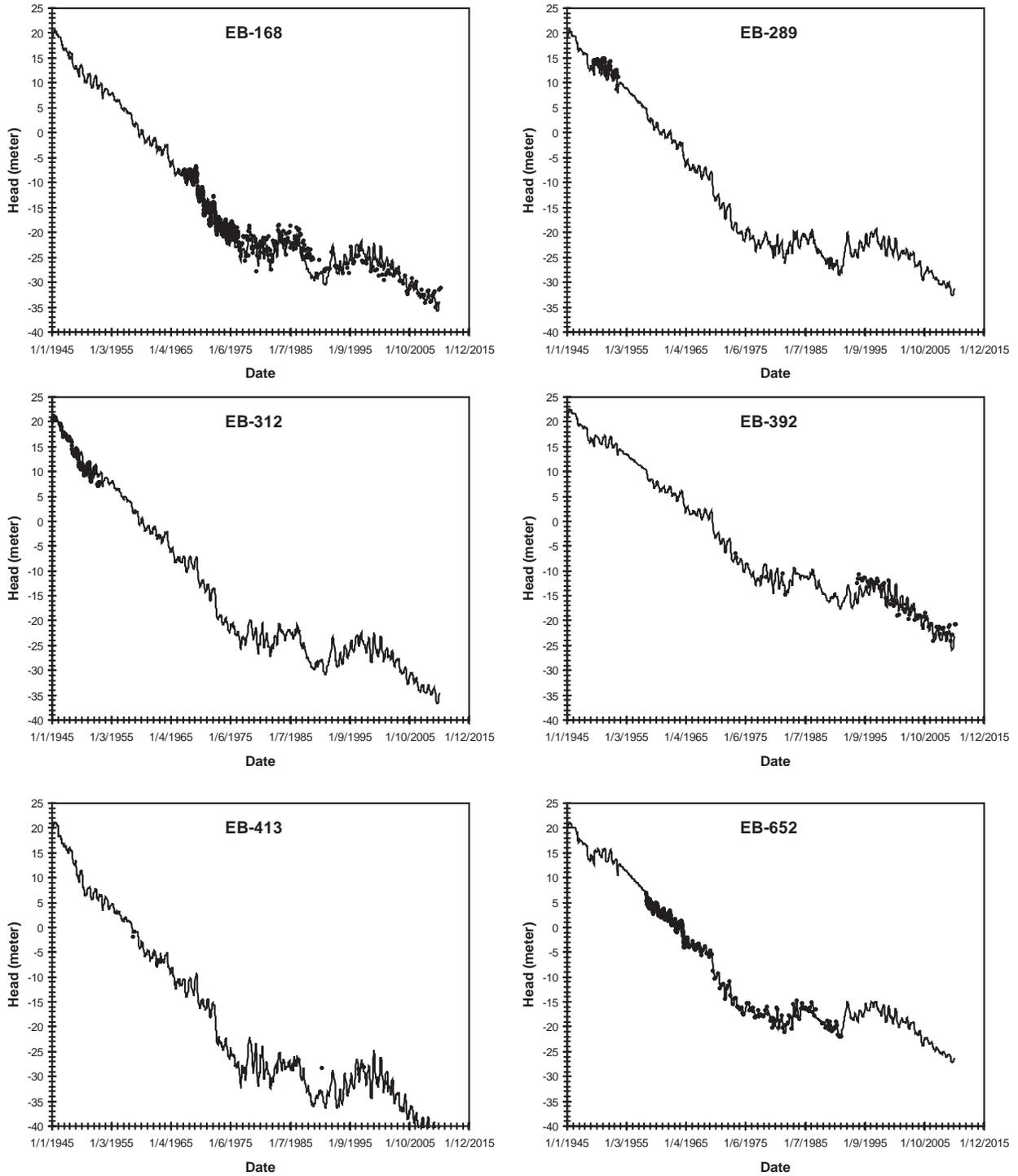
Figure 4: continued.
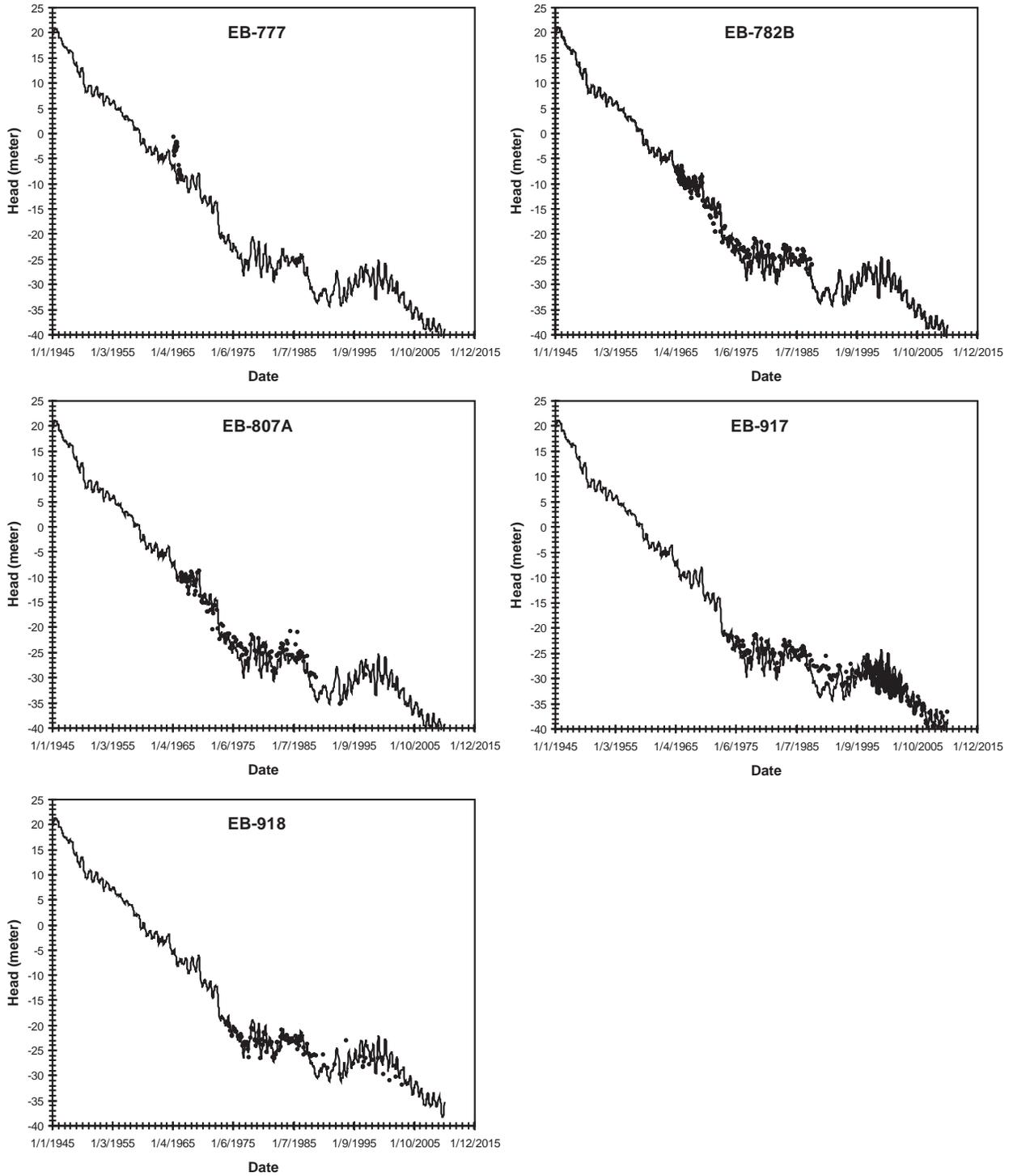
Figure 5: Simulated groundwater head (m) distribution on 1/1/2010.
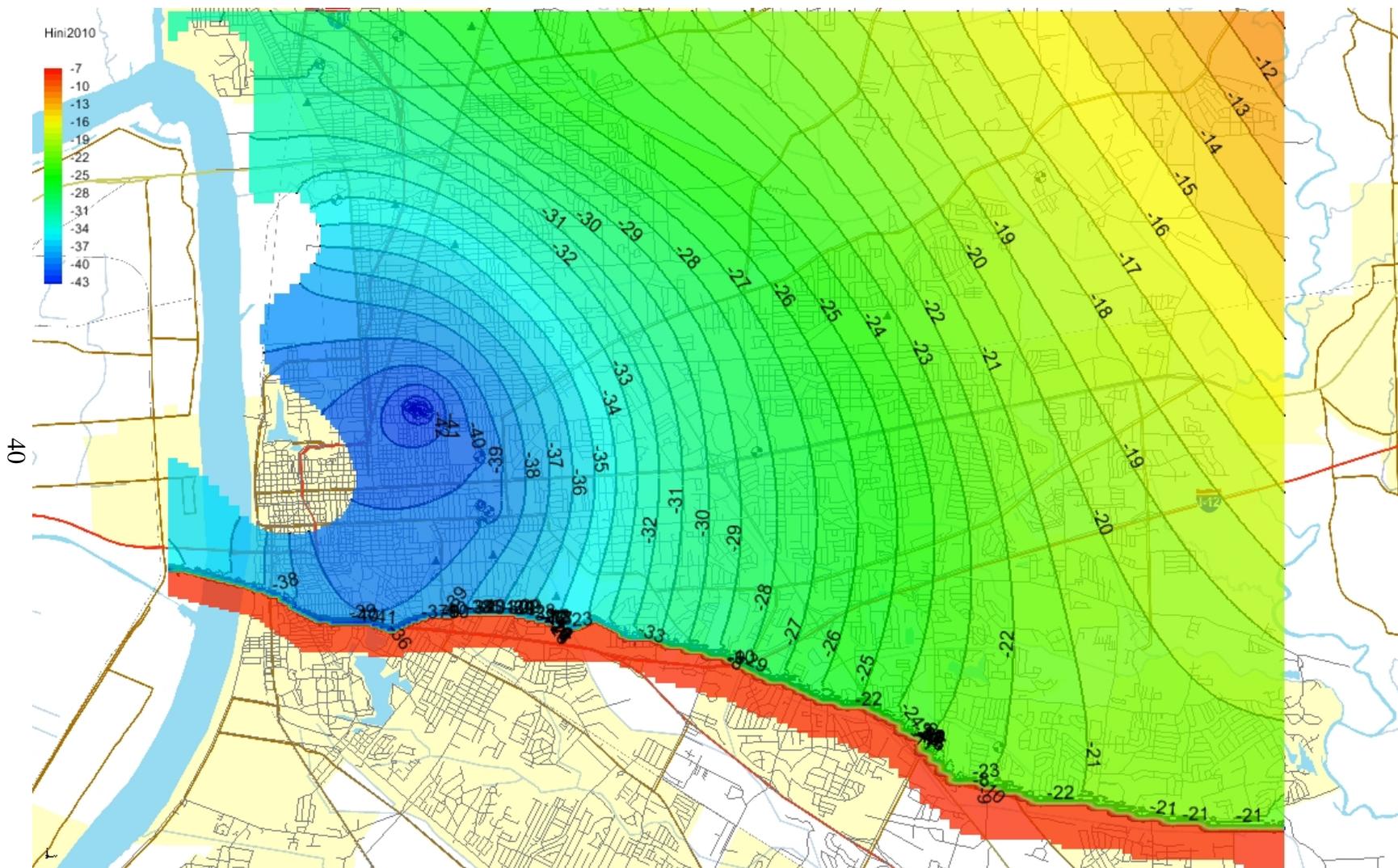
Figure 6: Simulated groundwater heads at EB-782B and at its adjacent computational cell (134, 71) south of the fault, pressure difference (psi), and flow velocity (m/day).
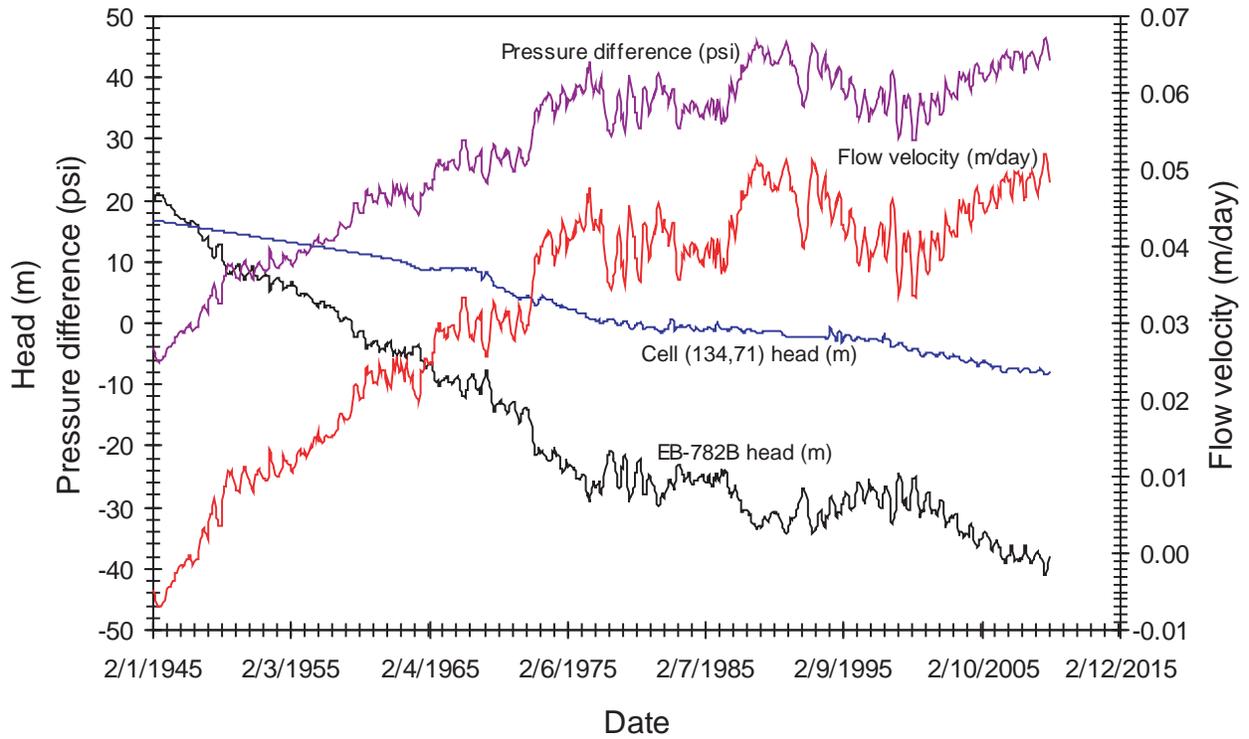
Figure 7: Calibration result of the MT3DMS model. Solid lines represent simulated chloride concentration and symbols represent chloride data.
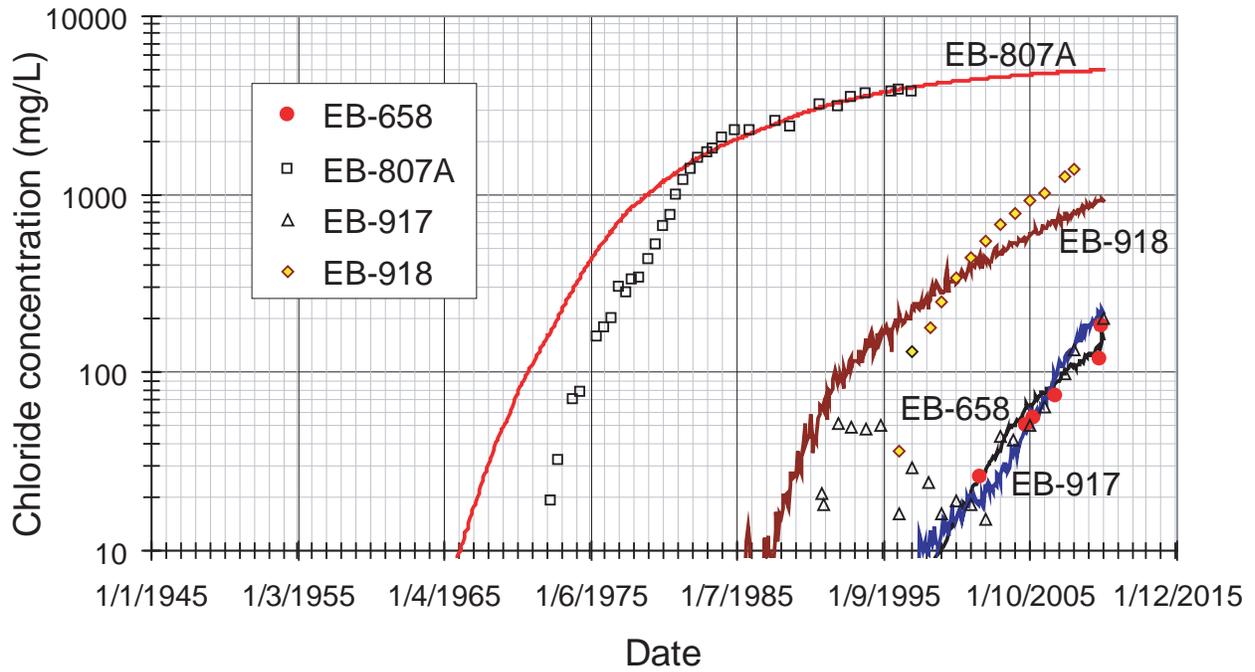
Figure 8: Saltwater intrusion pattern. Front line represents chloride concentration of 250 mg/L.
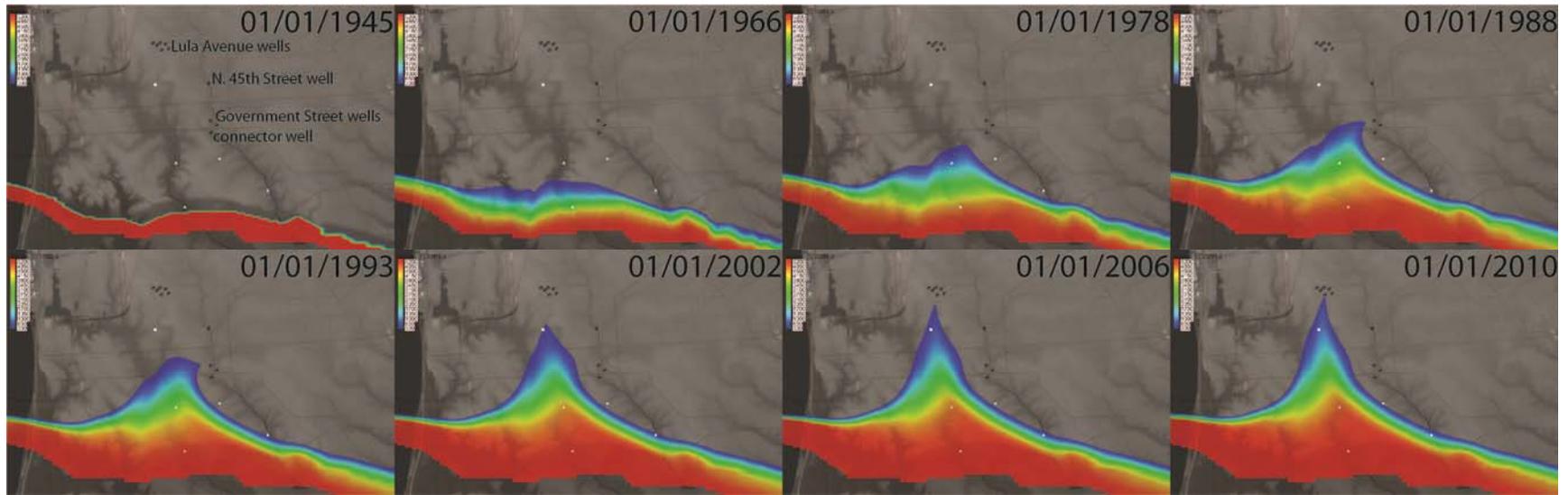
Figure 9: Simulated chloride concentration distribution on 1/1/2010. The front line is 250 mg/L.
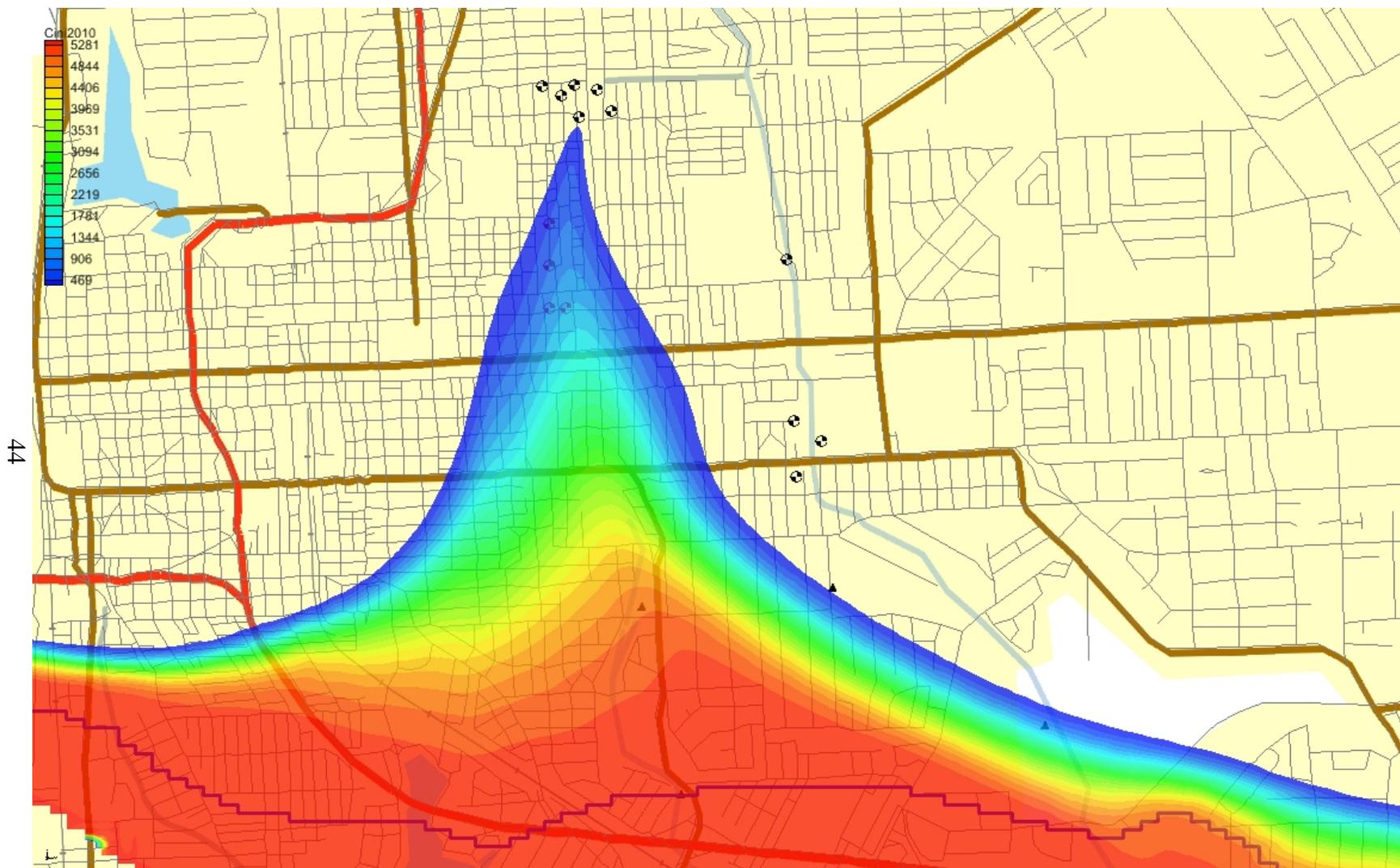
Figure 10: Simulated chloride concentration (mg/L) at EB-782B and at its adjacent computational cell (134, 71) south of the fault, advective chloride mass flux, dispersive chloride mass flux, and total chloride mass flux (kg/day-m^2).
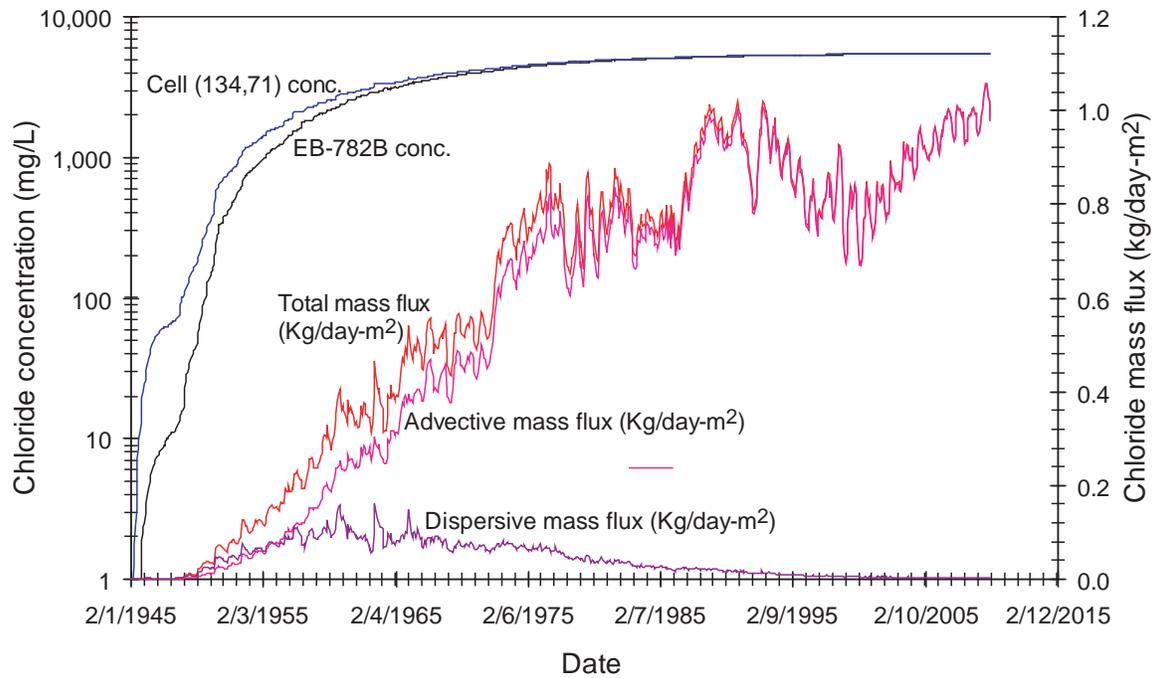
Figure 11: Simulated chloride concentrations without scavenger wells for the period 1/1/1945-12/31/2059 (the no-action scenario).
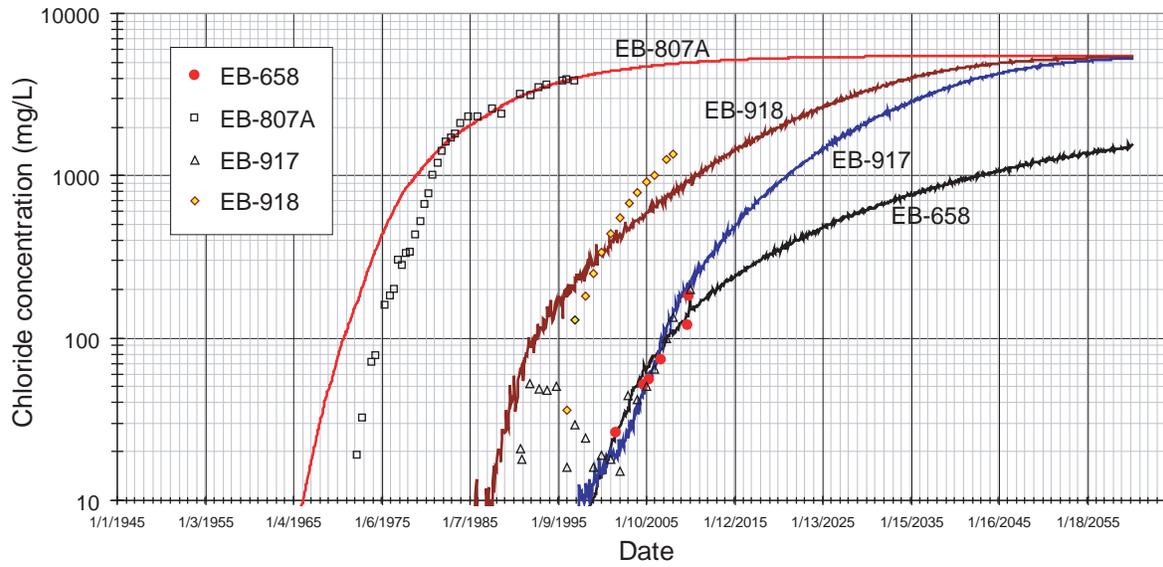
Figure 12: Chloride concentration distribution on (a) 1/1/2035, and (b) 1/1/2060 for the no-action scenario. The front line is 250 mg/L.
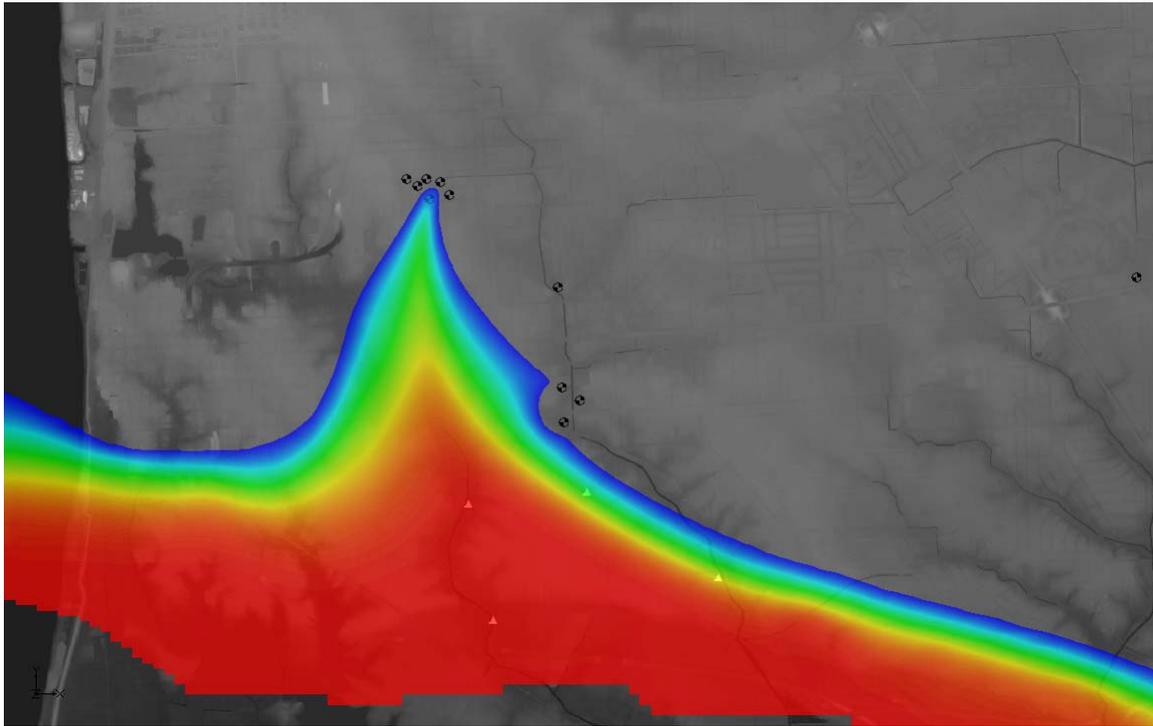
(a)
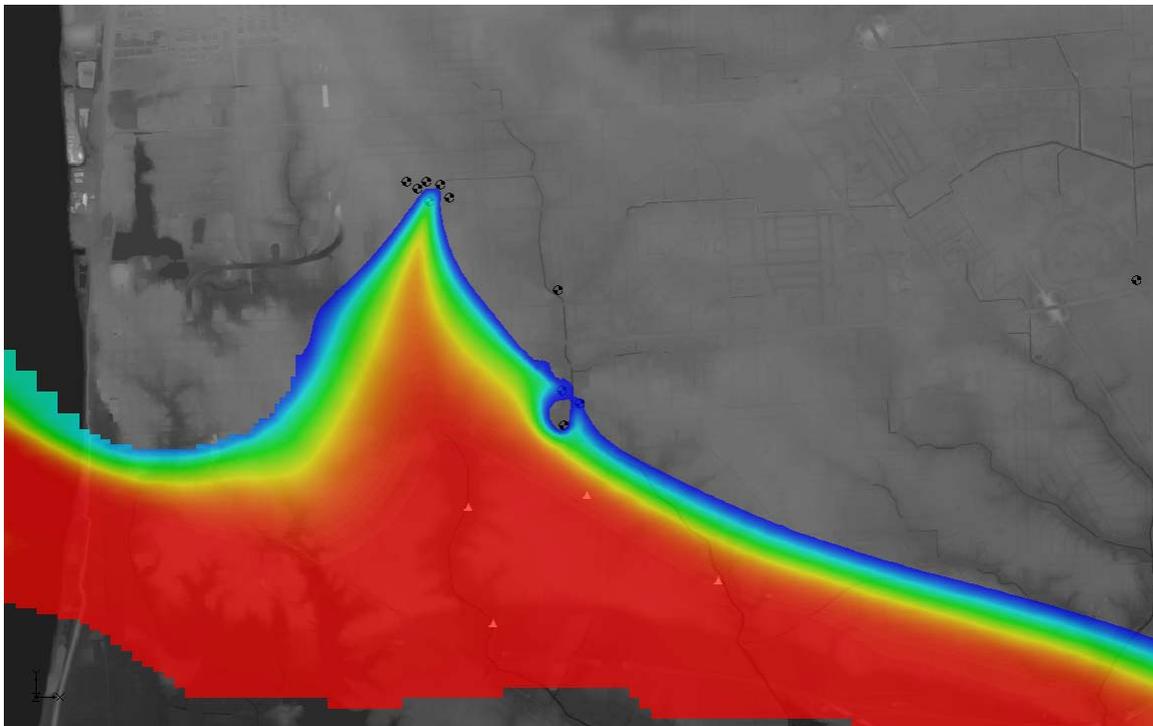
(b)

Figure 13: Scenario map.
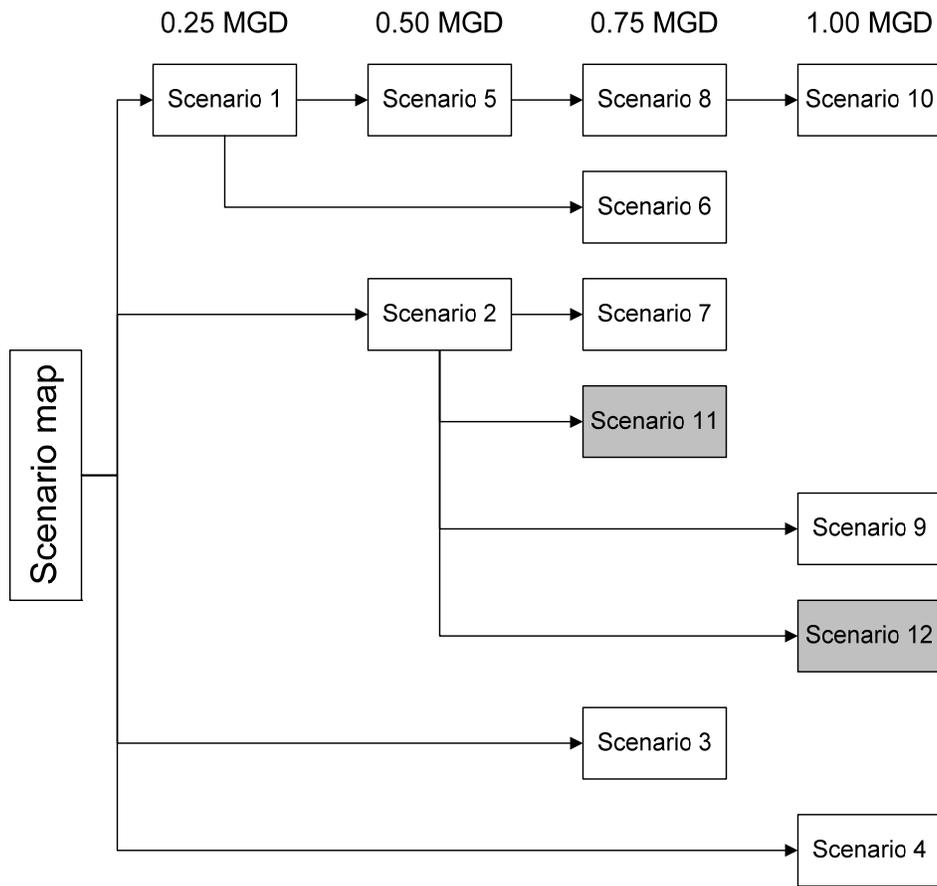
Figure 14: Potential location of scavenger wells and well numbers. EB-xxxx is a new observation well, being drilled to sample salinity.
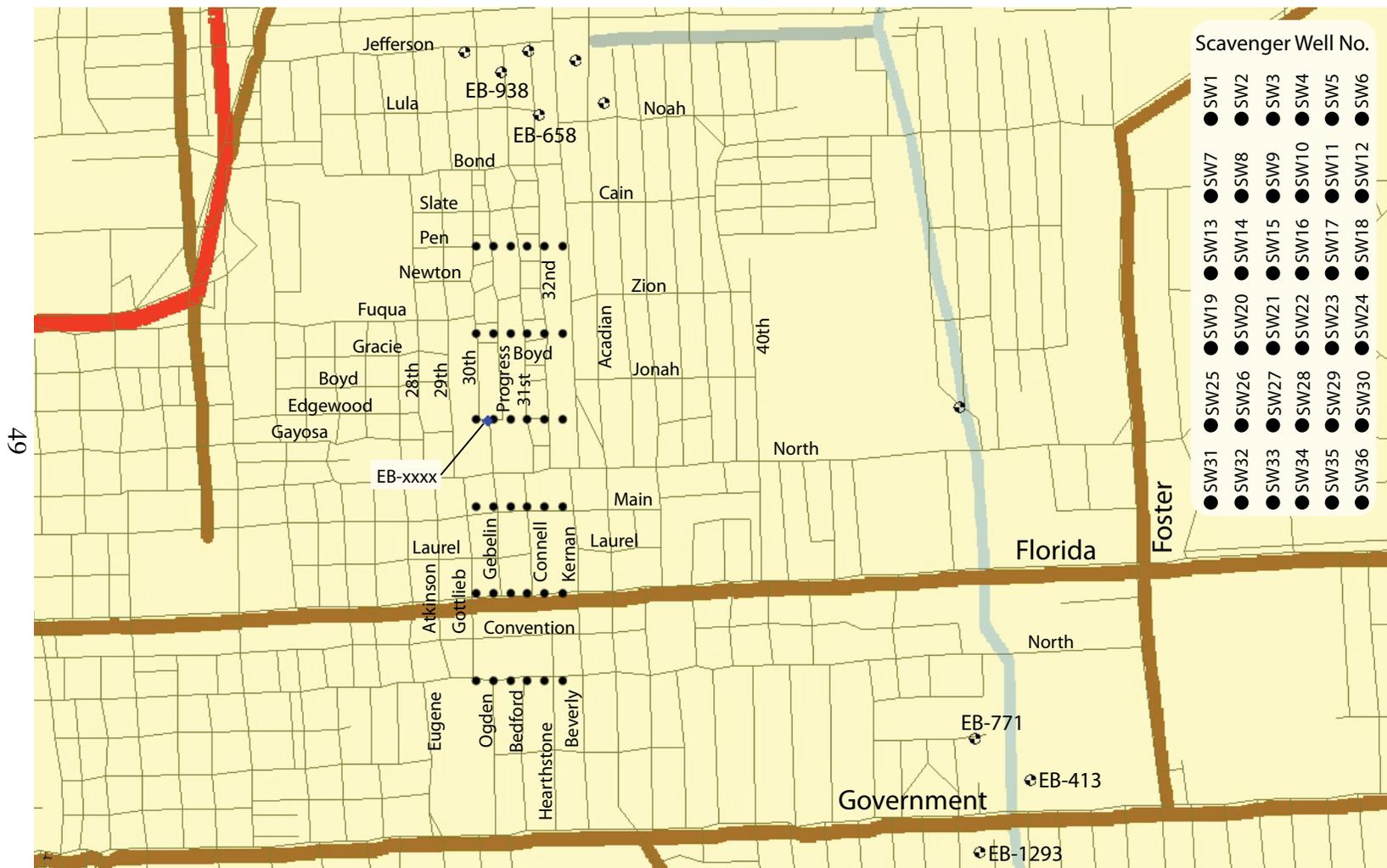
(Base Map obtained from Atlas: The Louisiana Statewide GIS, http://atlas.lsu.edu/)

Figure 15: Simulated chloride concentrations (mg/L) at EB-658 for different potential locations of a scavenger well in scenarios 1 to 4.
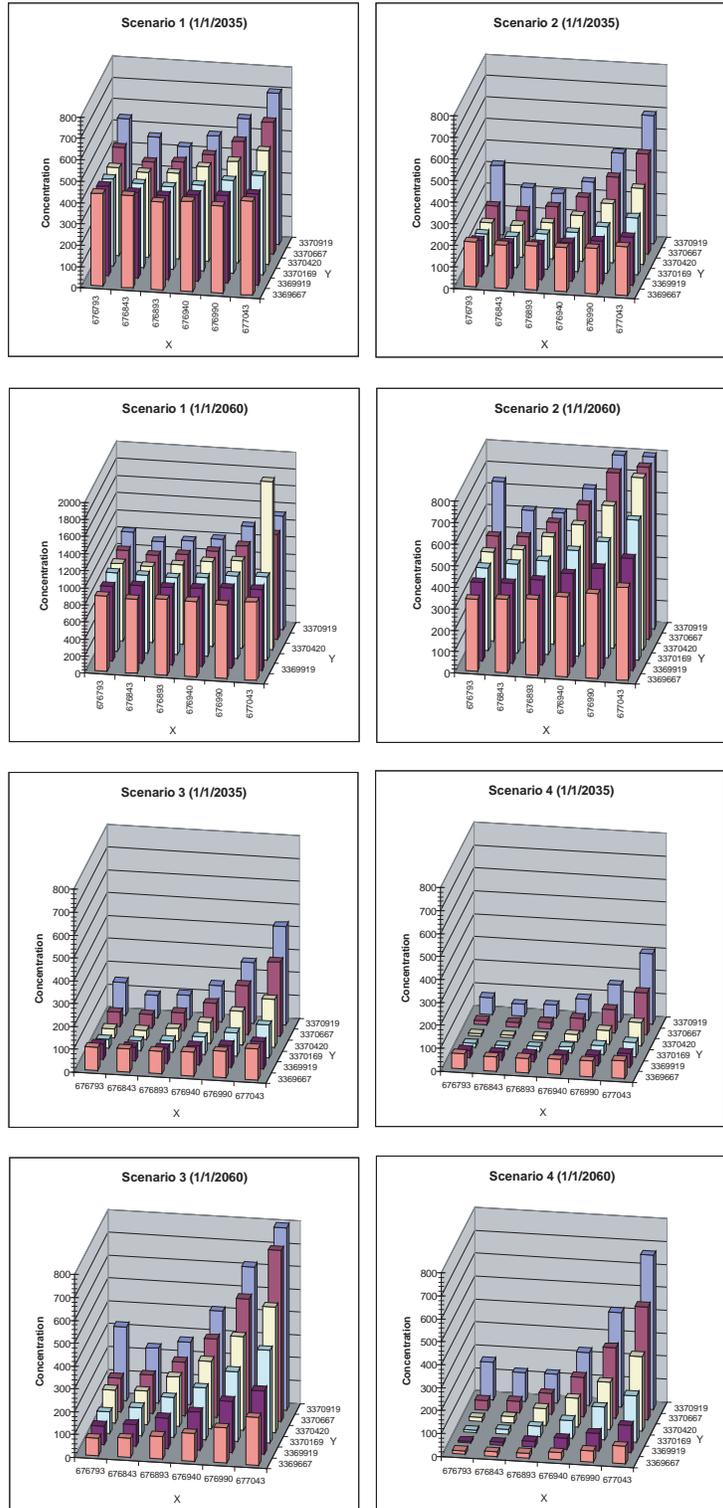
Figure 16: Simulated chloride concentration (mg/L) at EB-658 for different potential locations of the last scavenger well in scenarios 5 to 12.
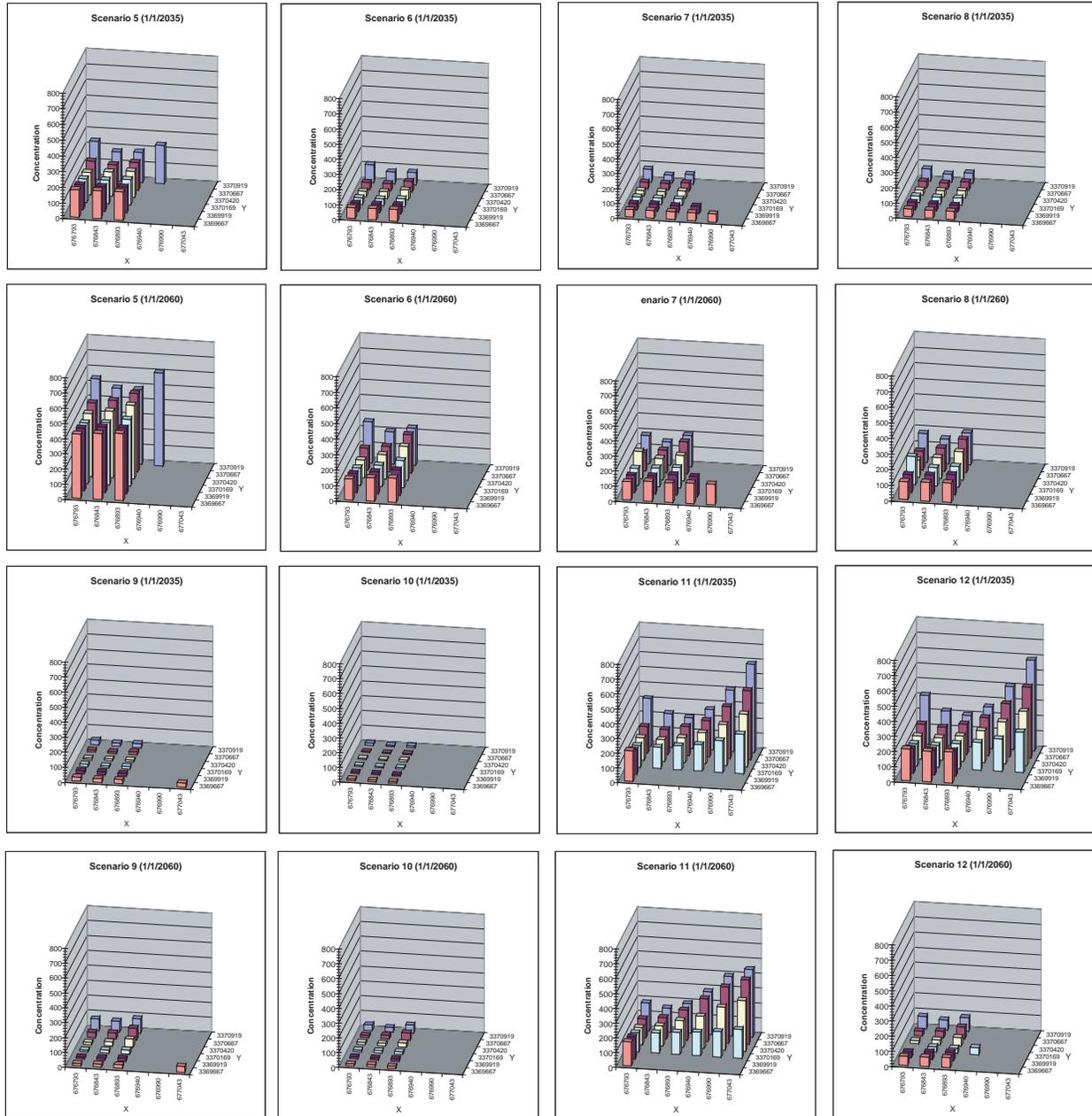
Figure 17: Predicted chloride concentration at EB-658 under different scenarios.

EB-658

Concentration (mg/L) vs Date

Labeled curves: 0.0 MGD, 0.25 MGD, 0.50 MGD, 0.75 MGD, 0.75 MGD, 1.00 MGD, 1.00 MGD, 0.75 MGD
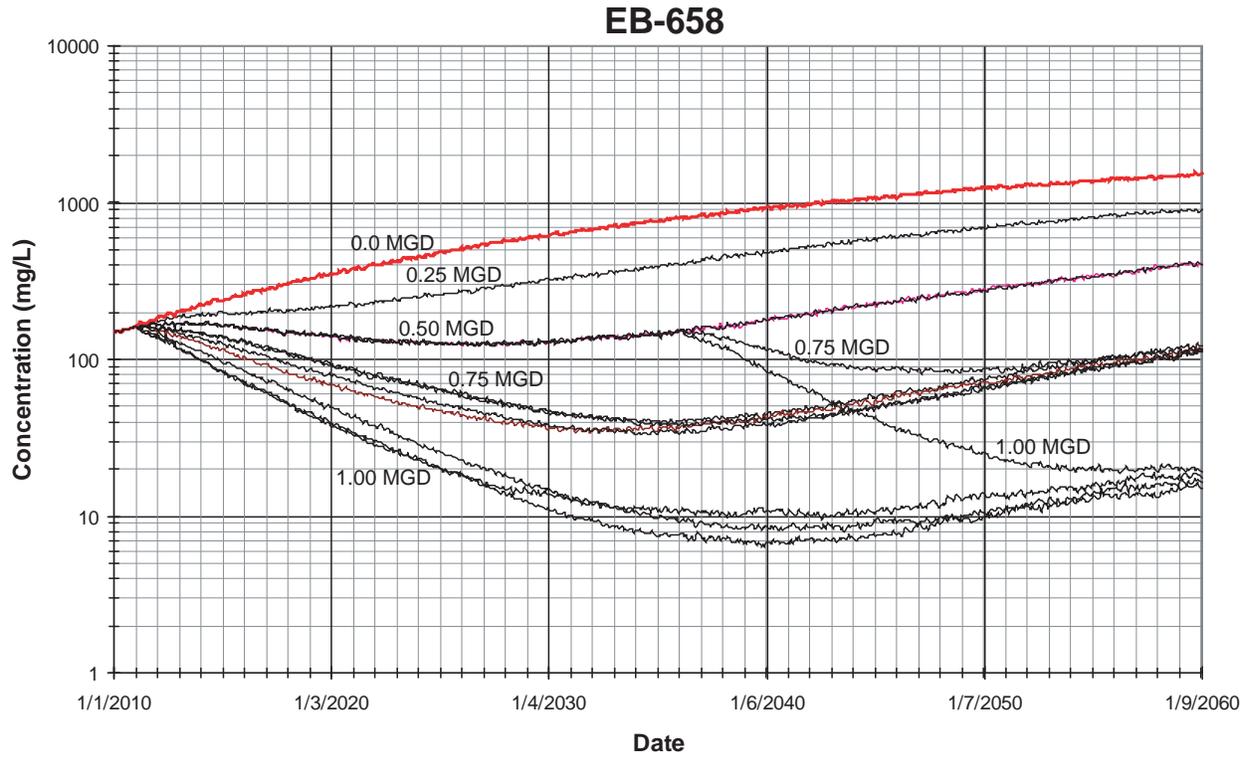
Figure 18: Predicted chloride concentrations at EB-807A, EB-917, and EB-918, EB-413 under different scenarios for the period 1/1/2010-12/31/2059.
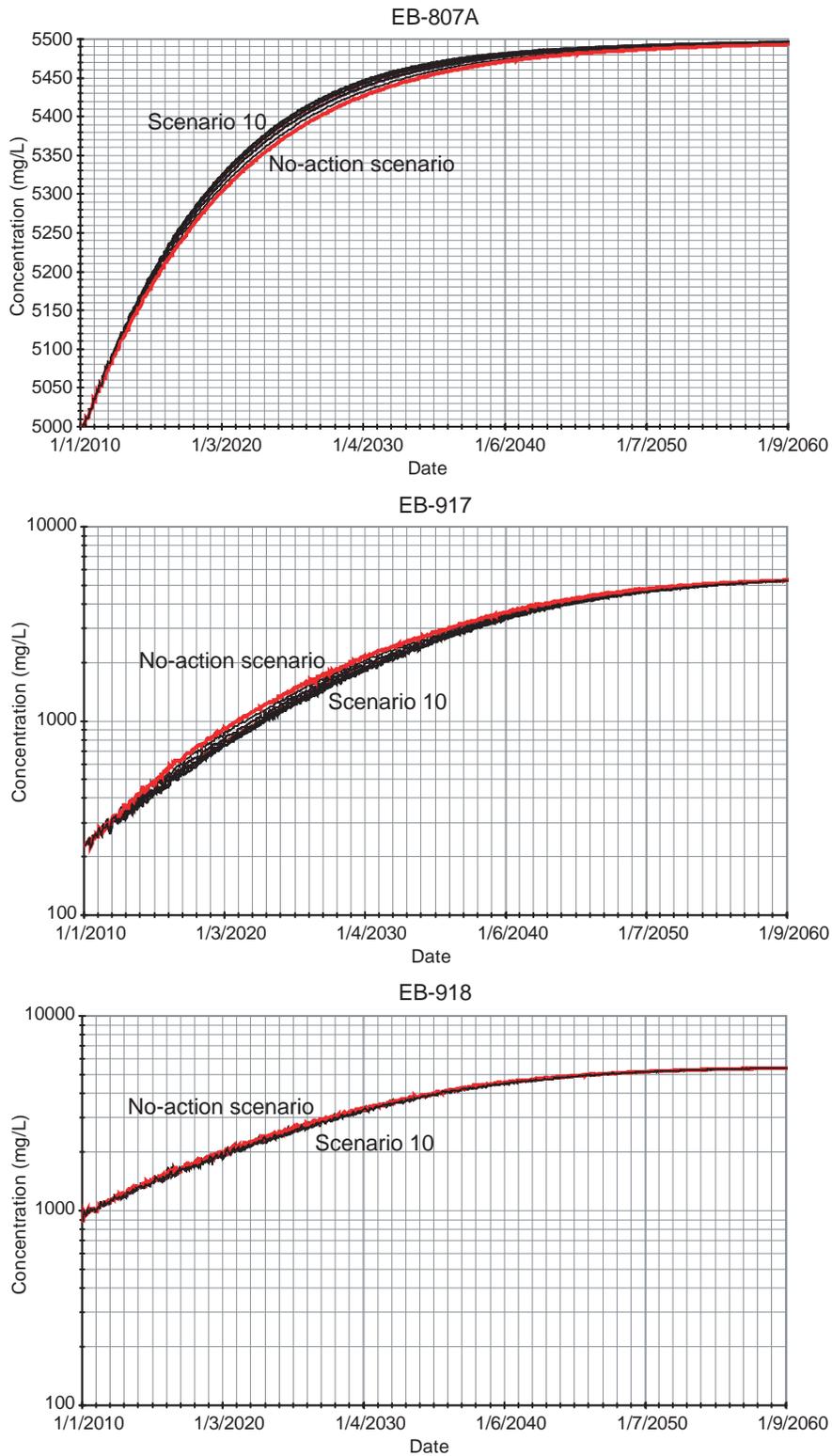
Figure 19: Predicted chloride concentrations at EB-413, EB-771, and EB-1293 under different scenarios for the period 1/1/2010-12/31/2059.
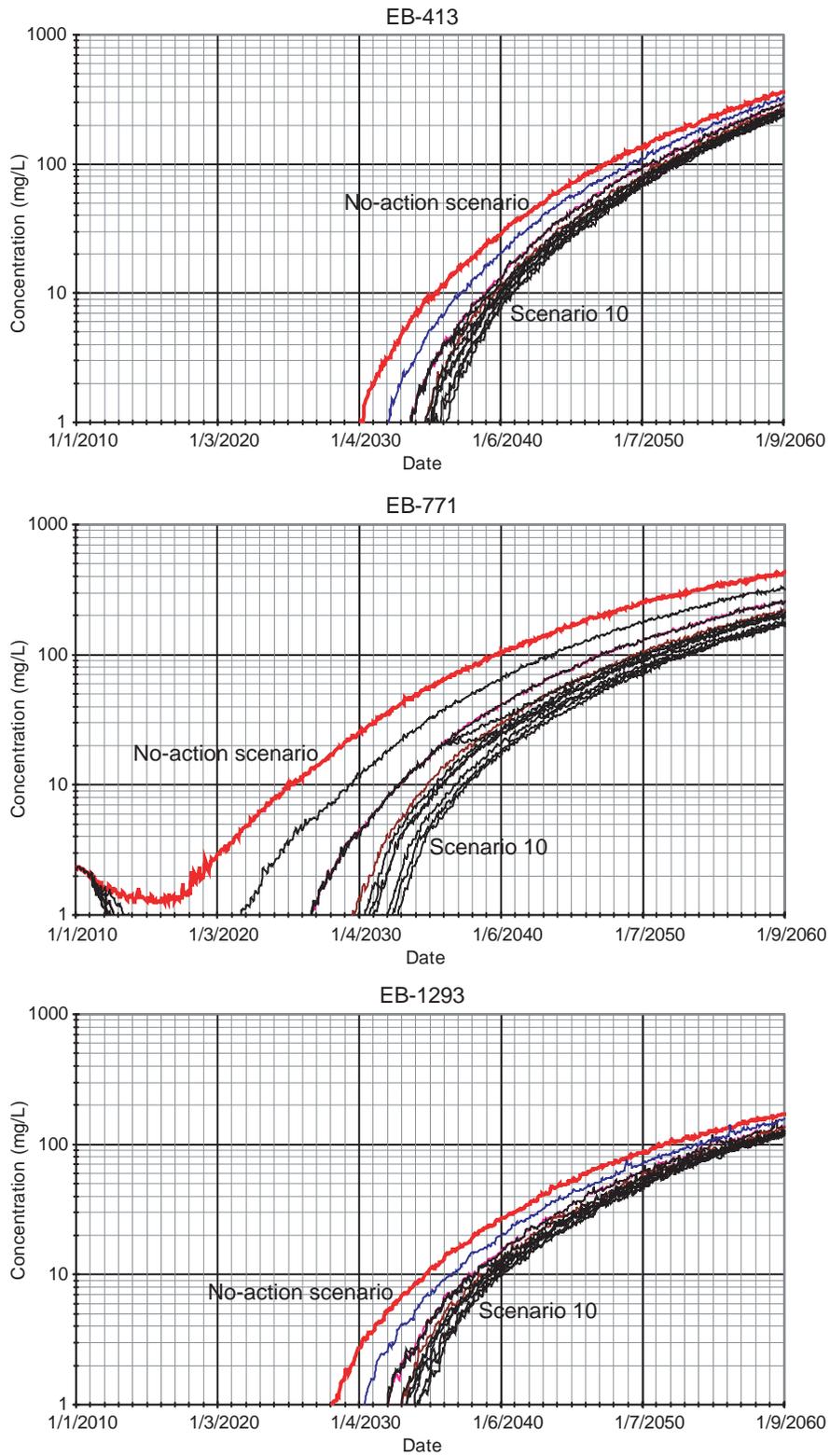
Figure 20: Simulated groundwater head at EB-782B and at its adjacent computational cell (134, 71) south of the fault, pressure difference (psi), and flow velocity (m/day) in the model calibration and model prediction periods for the no-action scenario and scenario 10.
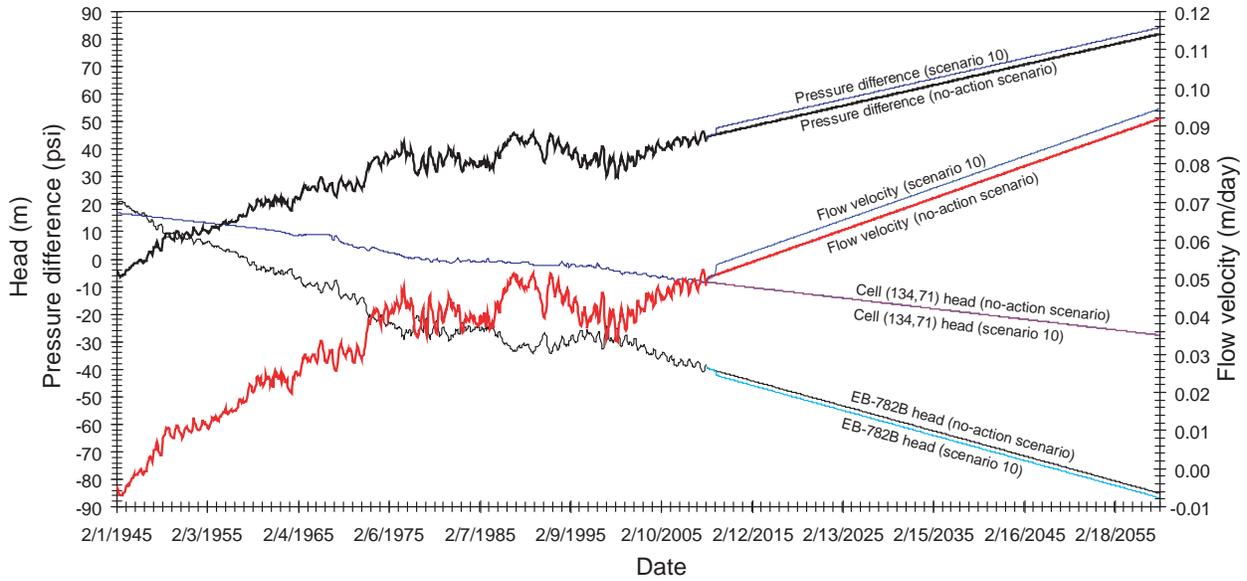
Figure 21: Simulated chloride concentrations (mg/L) at EB-782B and at its adjacent computational cell (134, 71) south of the fault, and total chloride mass flux (kg/day-m^2) in the model calibration and model prediction periods for the no-action scenario and scenario 10.
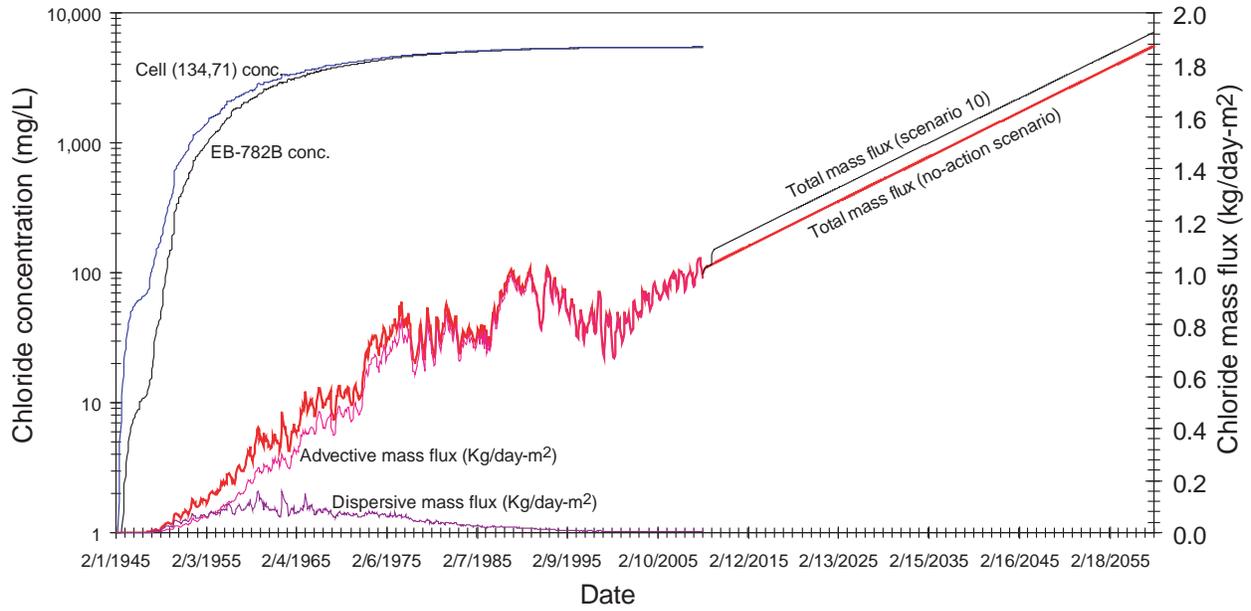
Figure 22: Chloride concentration distribution on 1/1/2035 under scenario 10. The front line is 250 mg/L.
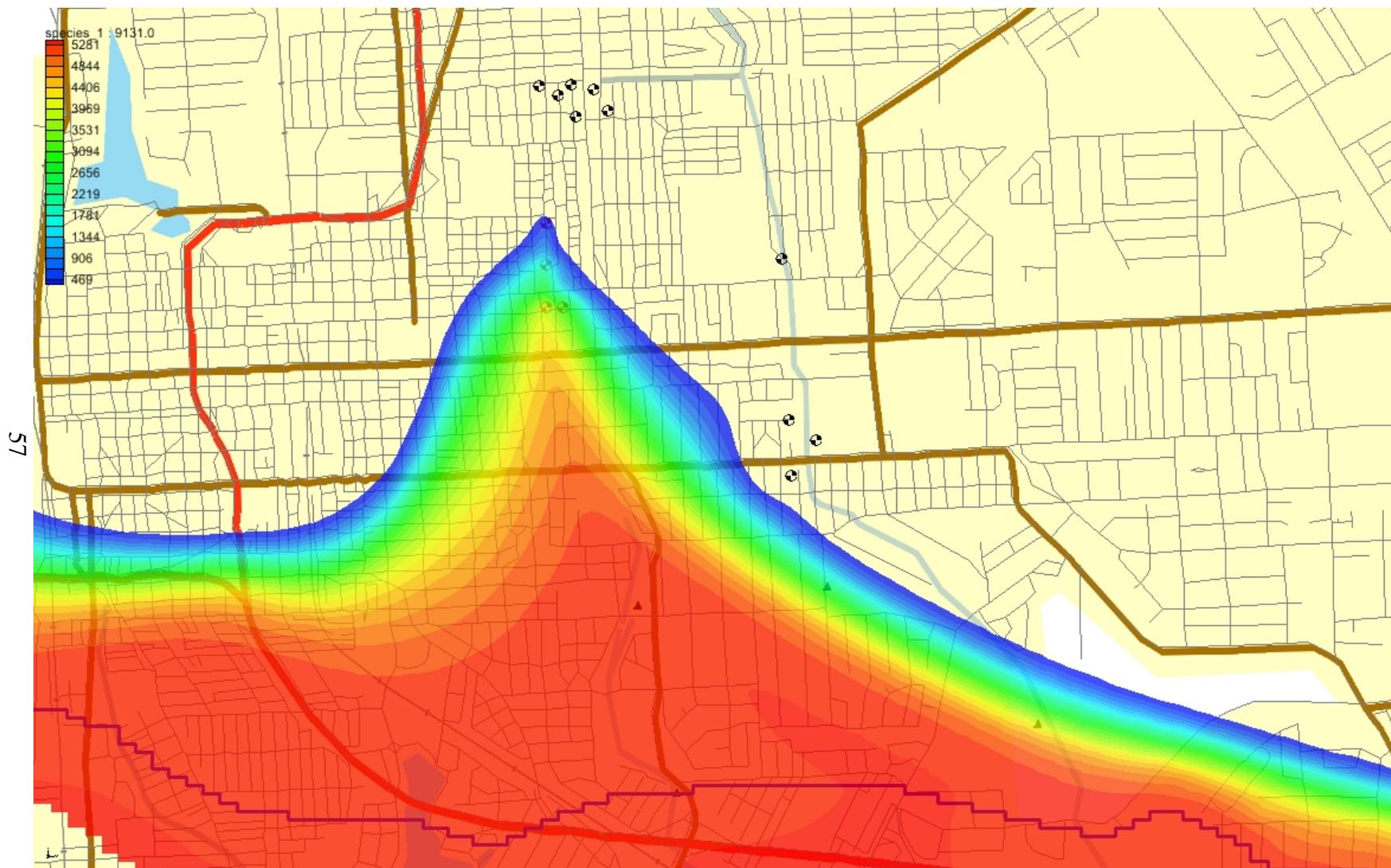
Figure 23: Chloride concentration distribution on 1/1/2060 under scenario 10. The front line is 250 mg/L.
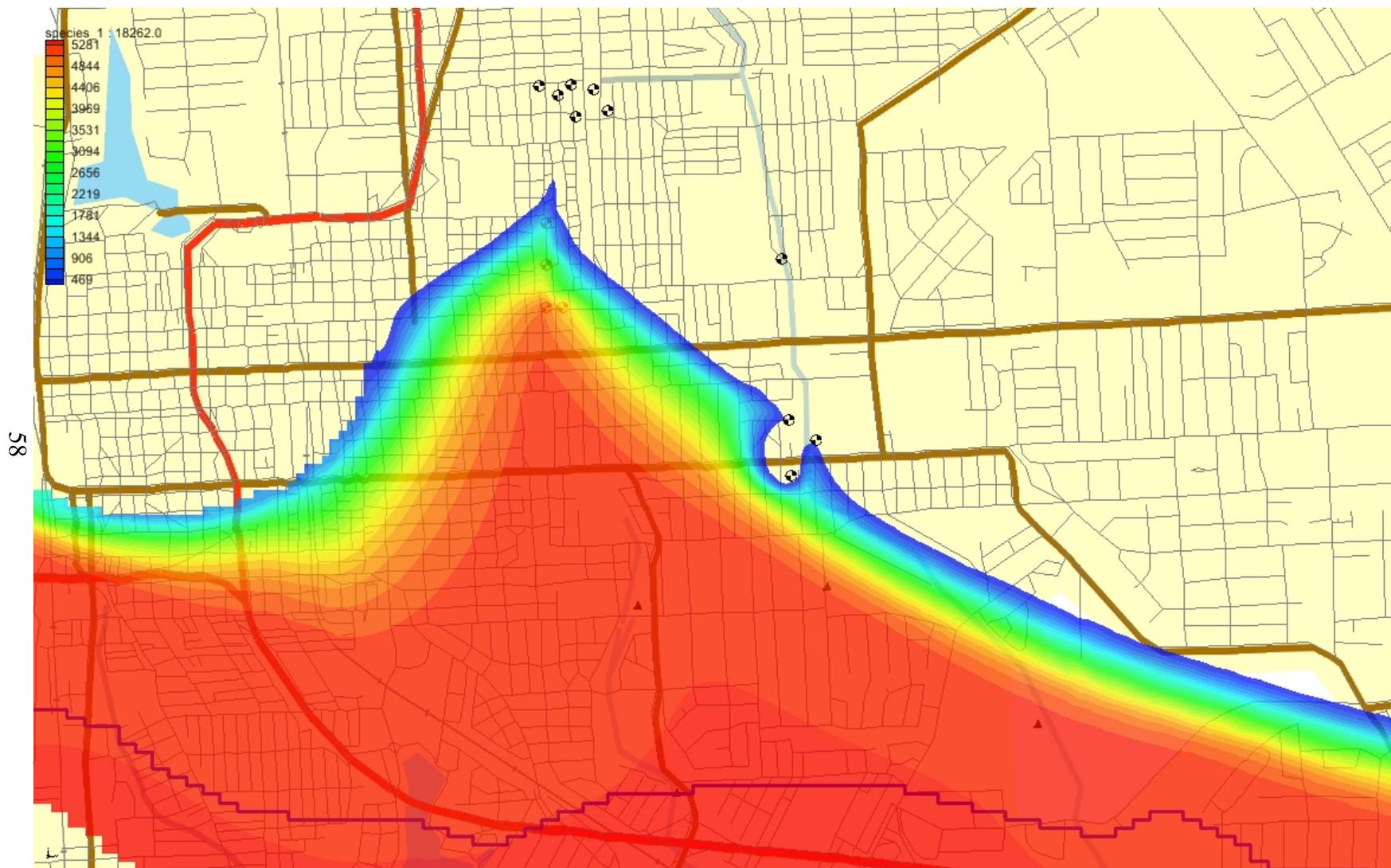
Figure 24: Extra drawdowns (meters) using scenario 4 with respect to the no-action scenario.
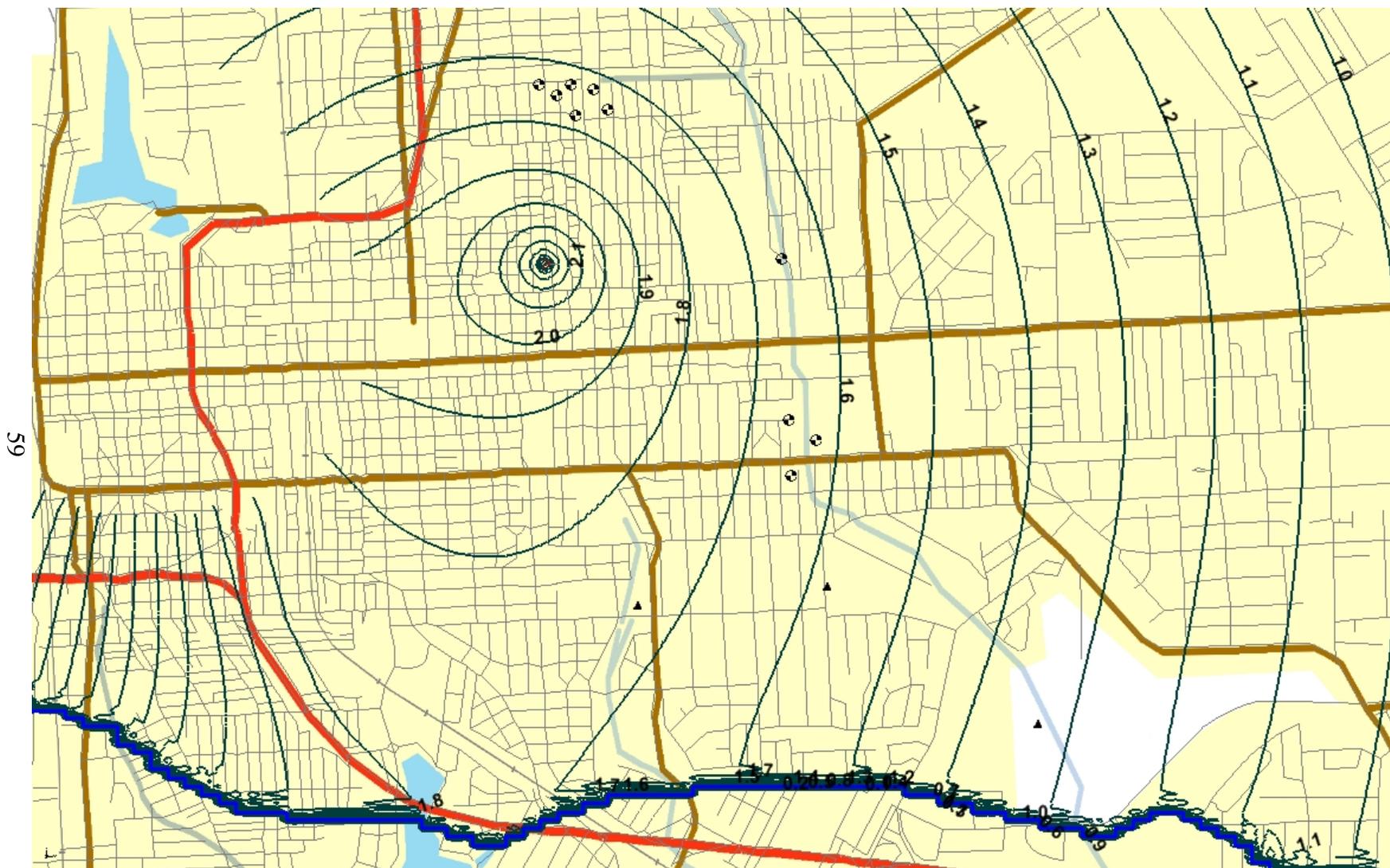
Figure 25: Extra drawdowns (meters) using scenario 9 with respect to the no-action scenario.
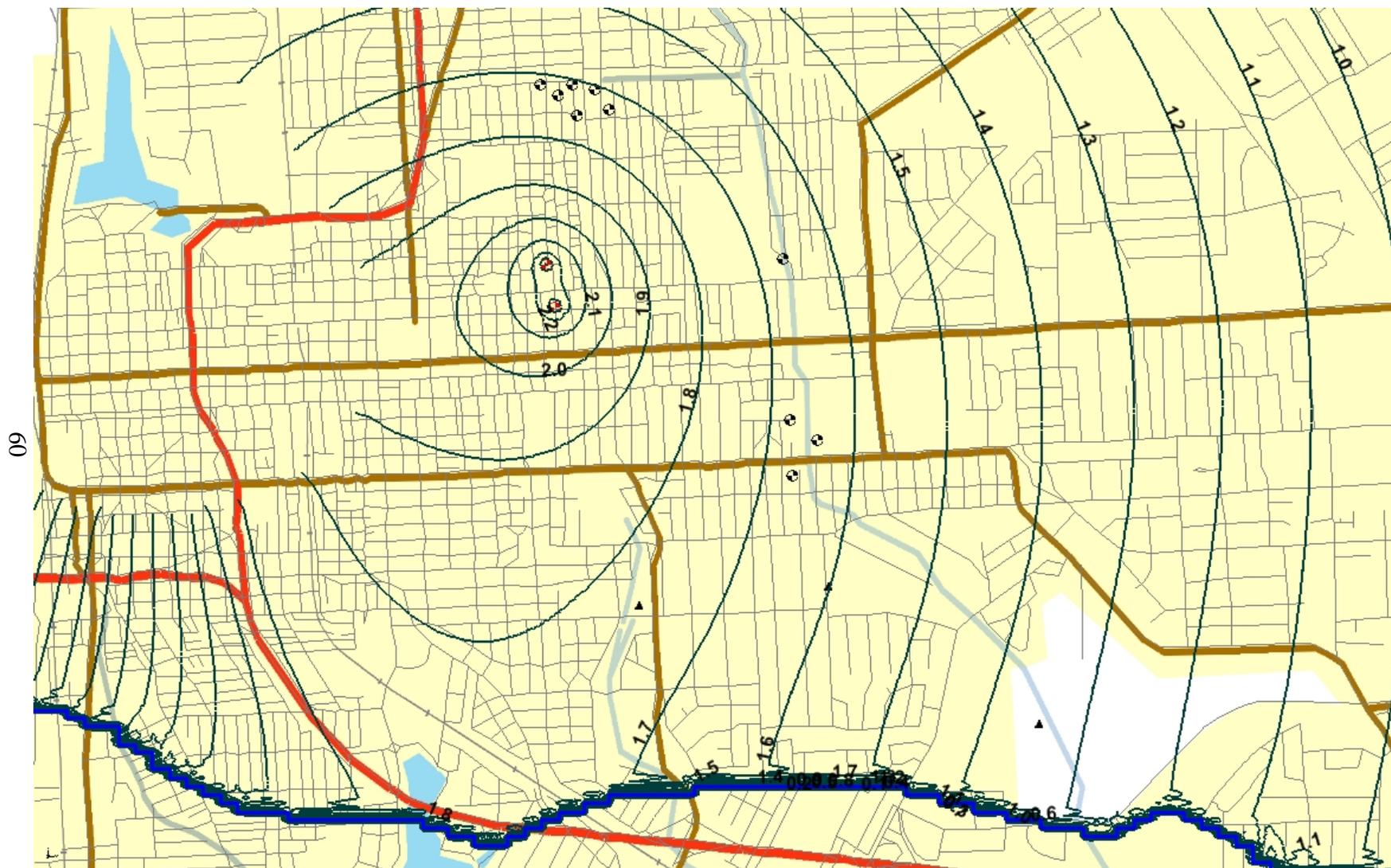
Figure 26: Extra drawdowns (meters) using scenario 10 with respect to the no-action scenario.
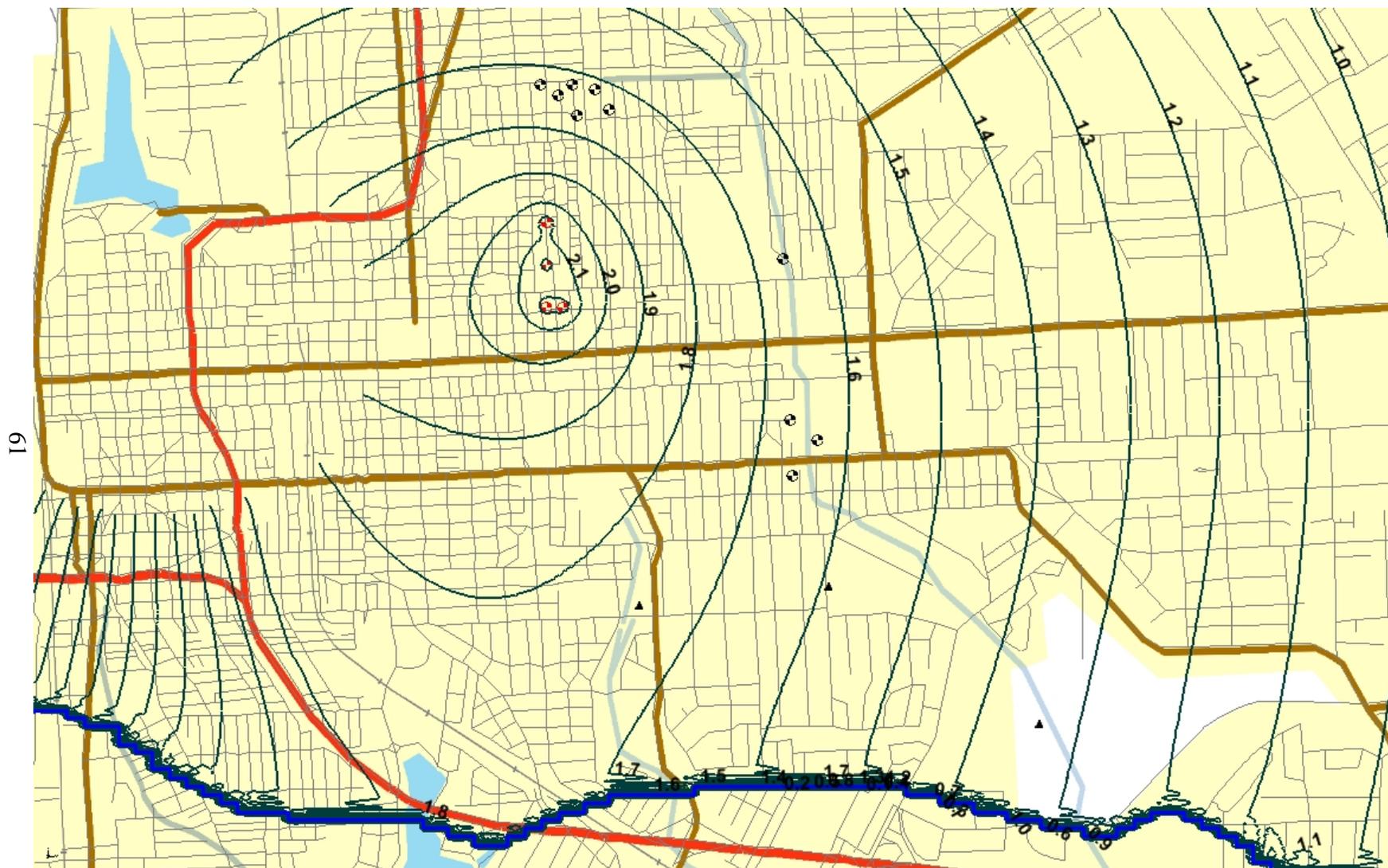
Figure 27: Calibration result of the MODFLOW model for the period 1/1/1945-12/31/2009, C_0=10,000 mg/L case. Lines represent simulated groundwater heads and filled circles represent head data.
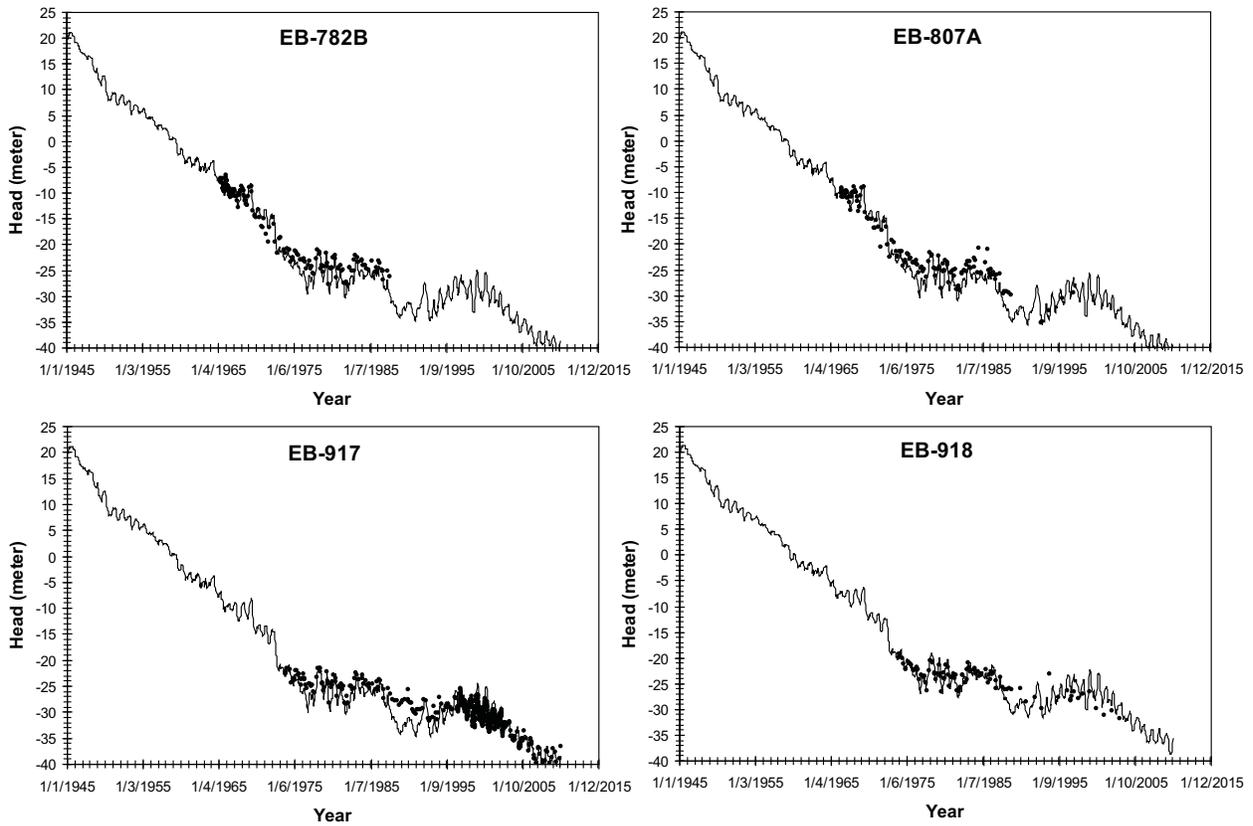
Figure 28: Calibration result of the MT3DMS model, C_0=10,000 mg/L case. Solid lines represent simulated chloride concentration and symbols represent chloride data.
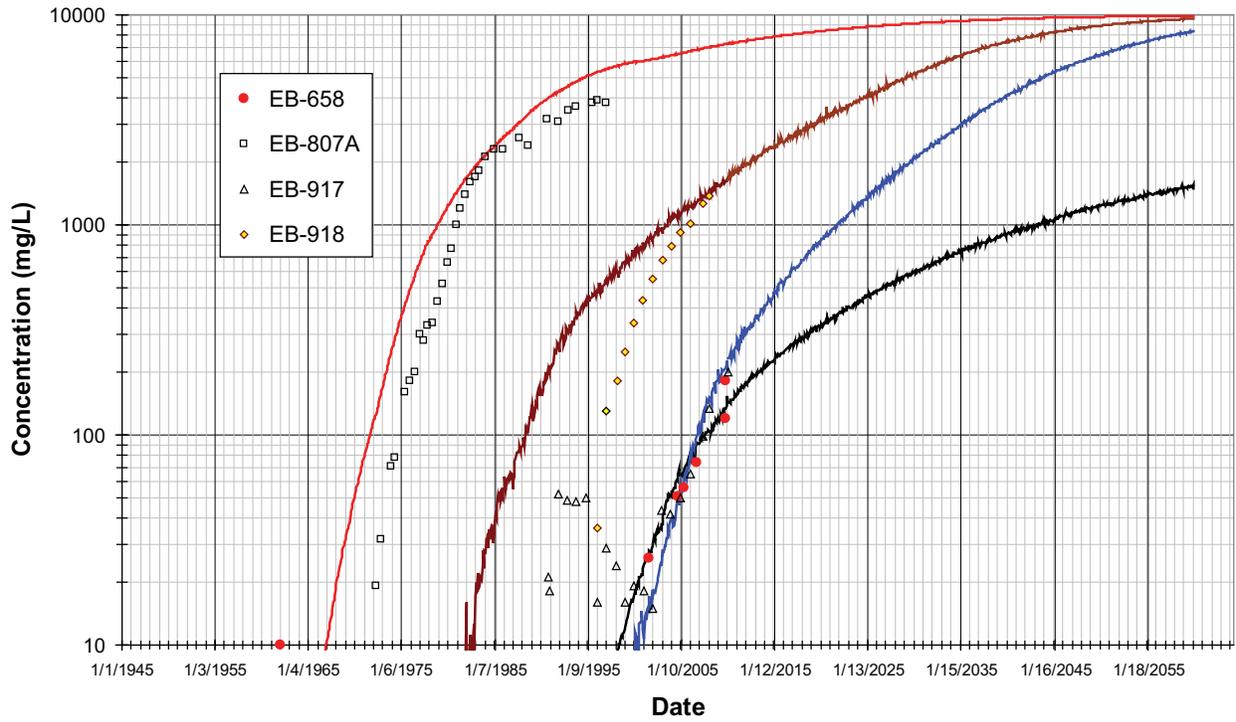
Figure 29: Predicted chloride concentration at EB-658, C_0=10,000 mg/L case.
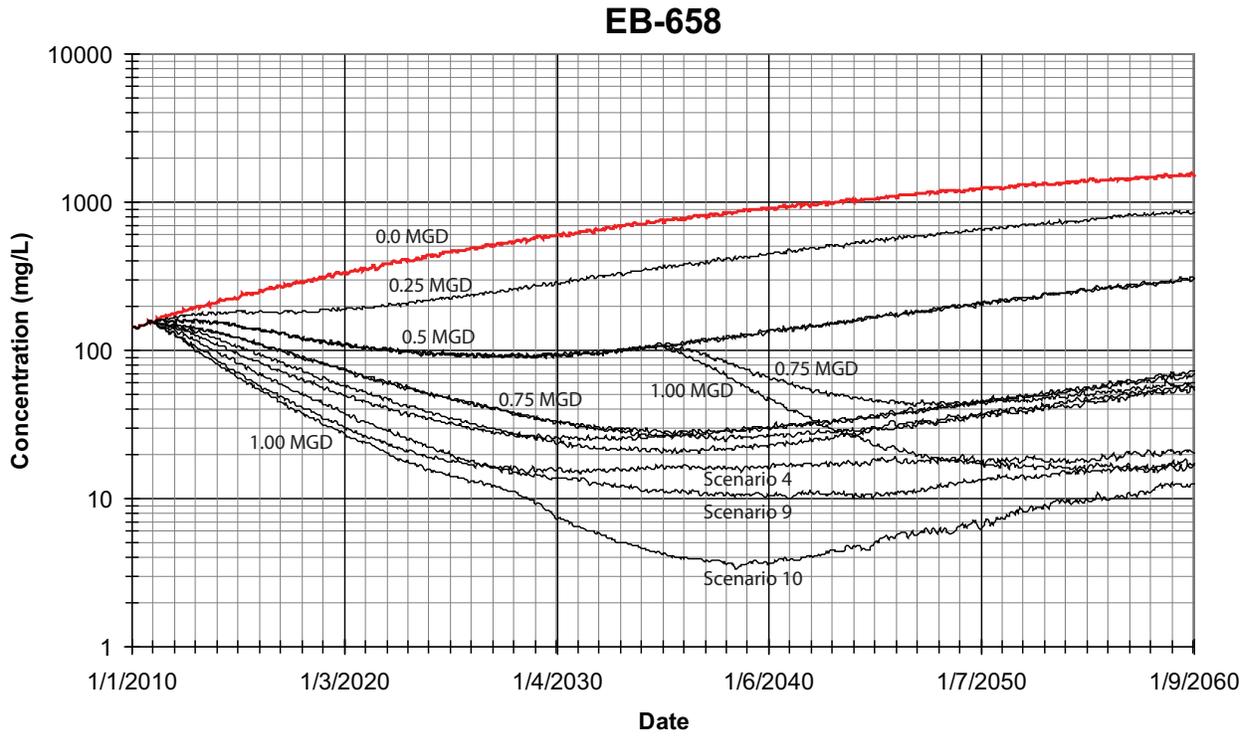
Figure 30: Chloride concentration distribution on 1/1/2010, C_0=10,000 mg/L case. The front line is 250 mg/L.
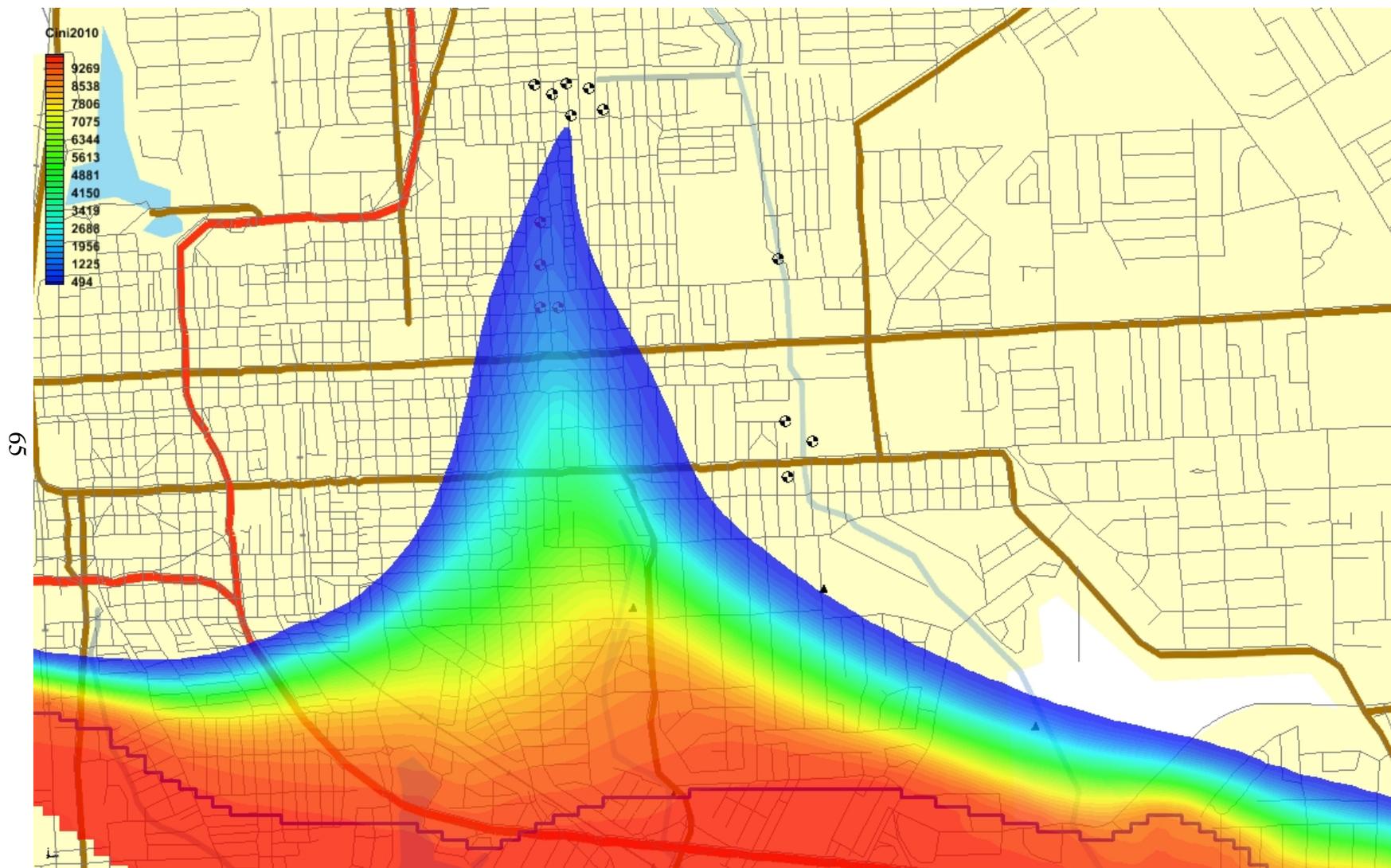
Figure 31: Chloride concentration distribution on 1/1/2035 under scenario 10, C_0=10,000 mg/L case. The front line is 250 mg/L.
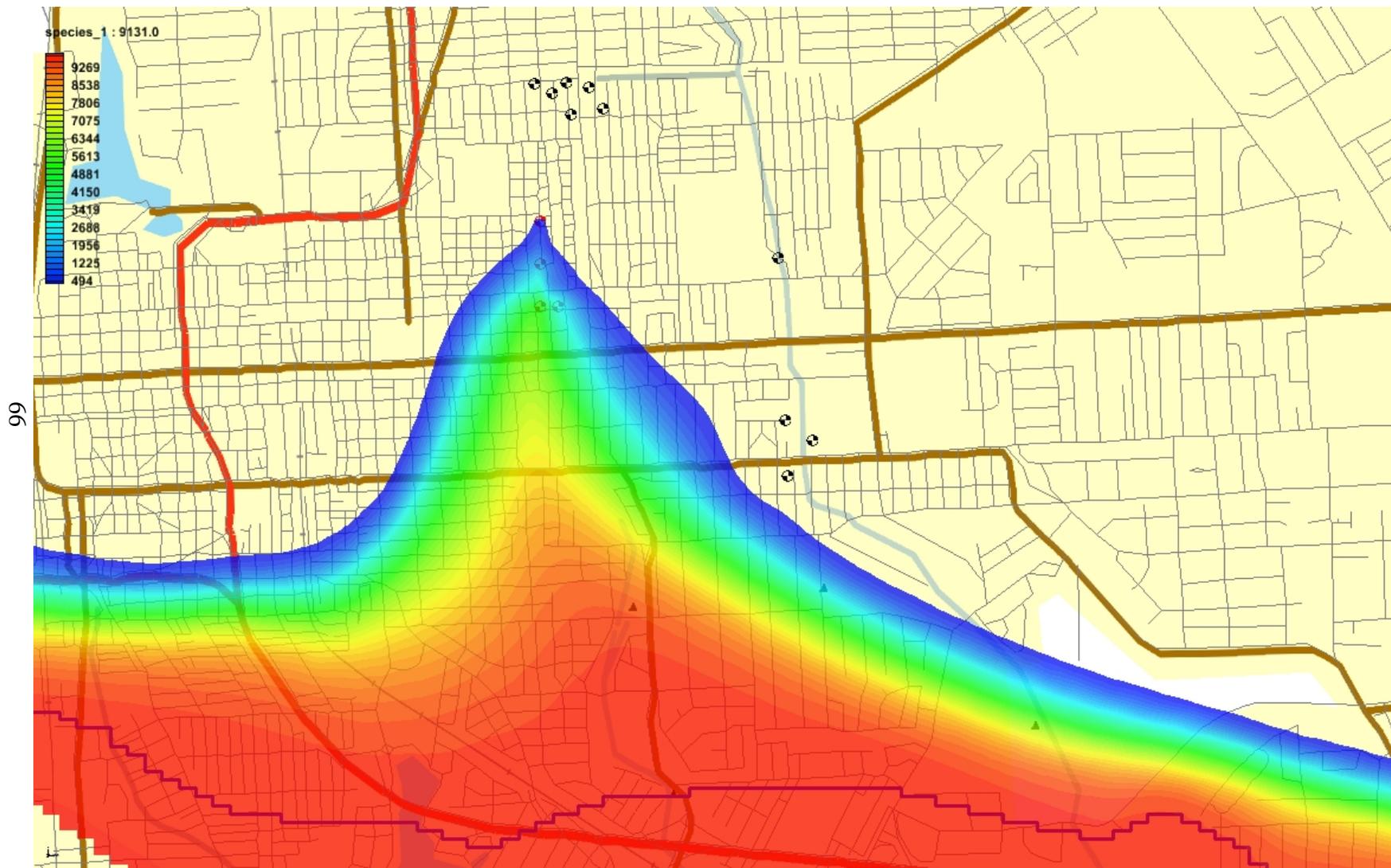
Figure 32: Chloride concentration distribution on 1/1/2060 under scenario 10, C_0=10,000 mg/L case. The front line is 250 mg/L.
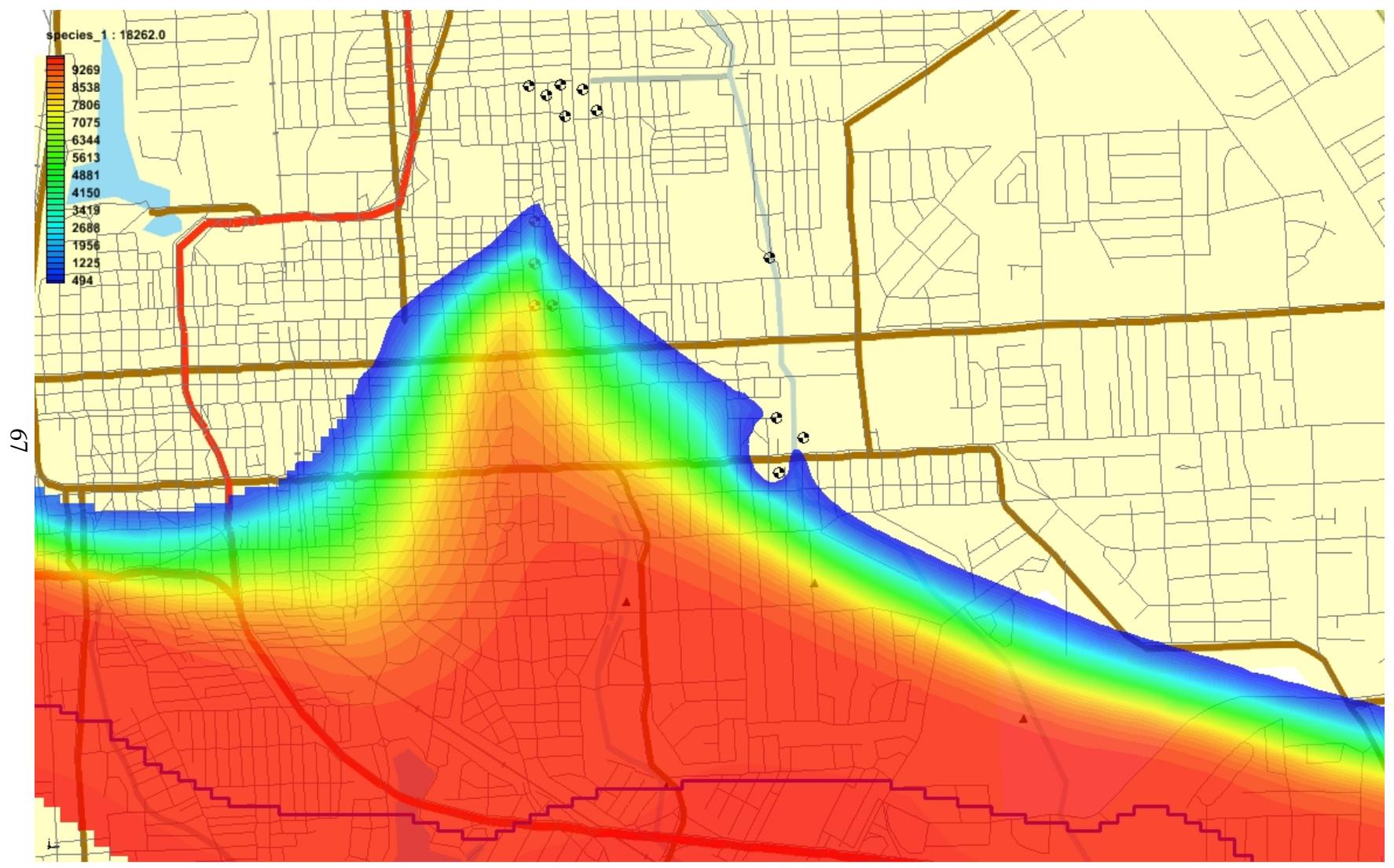
Figure 33: Extra drawdowns (meters) using scenario 4 with respect to the no-action scenario, C_0=10,000 mg/L case.
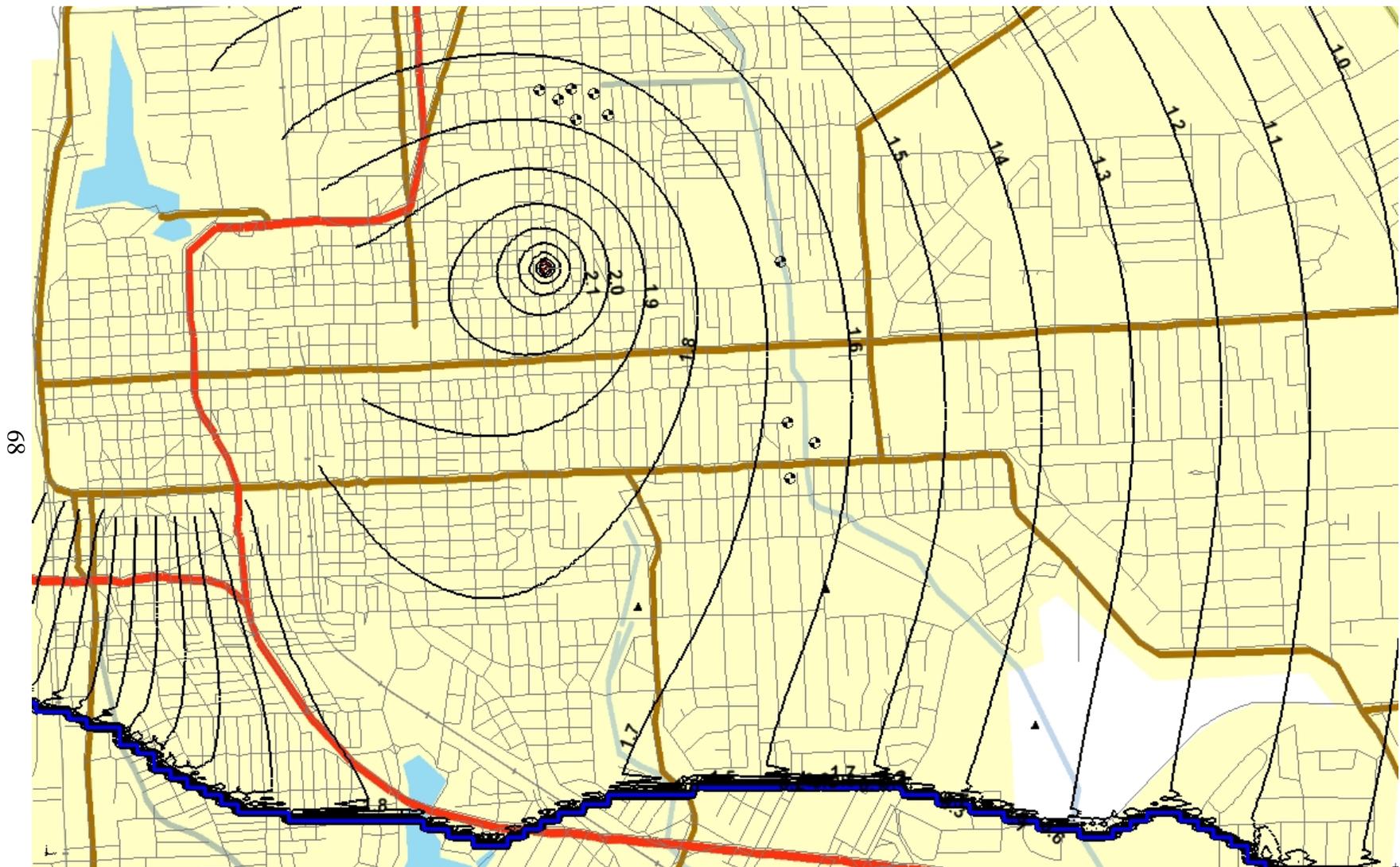
Figure 34: Extra drawdowns (meters) using scenario 9 with respect to the no-action scenario, C_0=10,000 mg/L case.
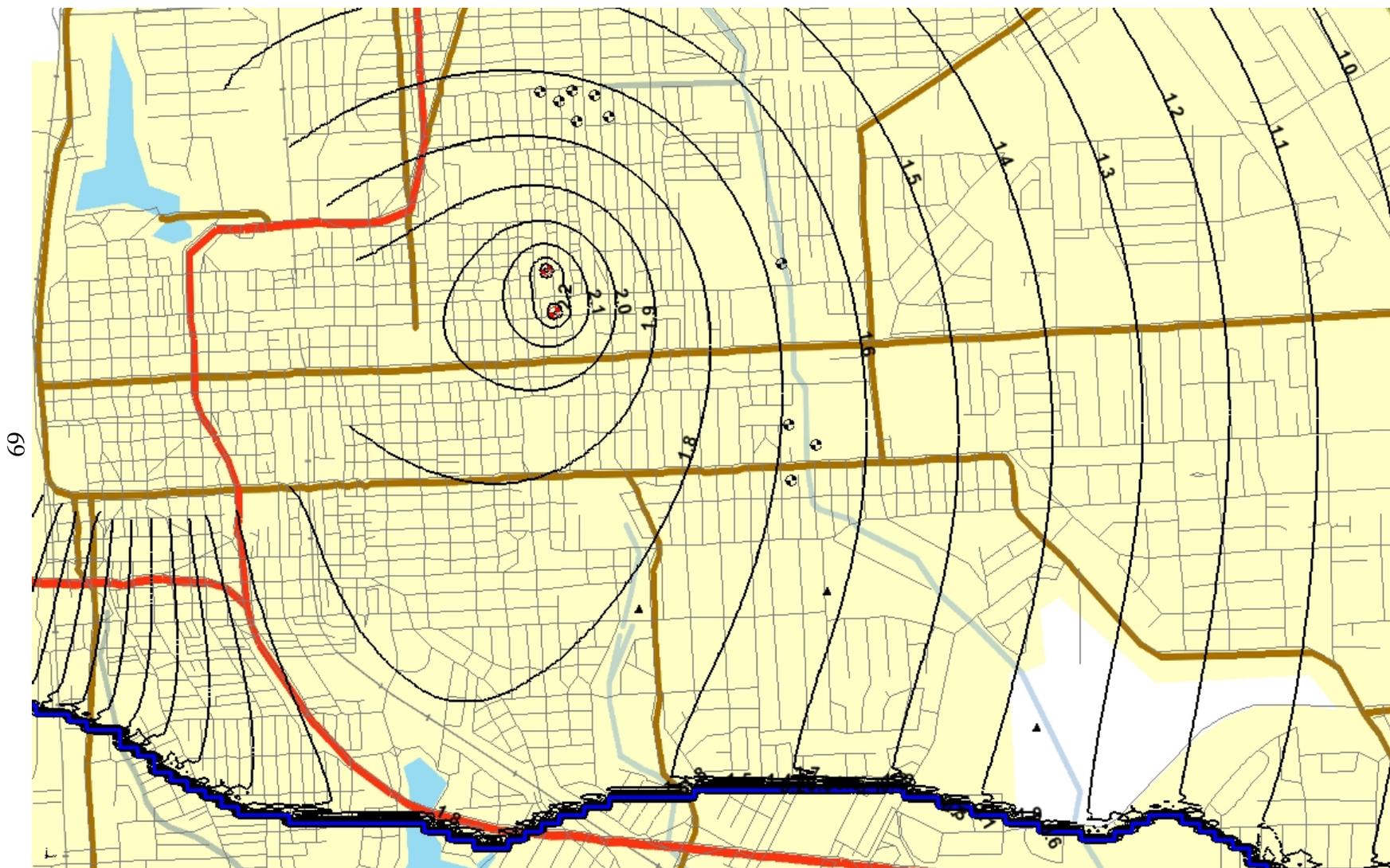
Figure 35: Extra drawdowns (meters) using scenario 10 with respect to the no-action scenario, C_0=10,000 mg/L case.